UNIVERSIDADE DE LISBOA
FACULDADE DE CIÊNCIAS
DEPARTAMENTO DE BIOLOGIA VEGETAL

Novel Regulators of Telomerase-Independent Telomere Elongation in ALT Cancer Cells

Beatriz Pedrosa Moleirinho

Mestrado em Biologia Molecular e Genética

Dissertação orientada por:
Claus M. Azzalin
Rita Zilhão

2020

Acknowledgements

I would like to extend my sincere gratitude to Professor Dr. Claus M. Azzalin, my supervisor at Instituto de Medicina Molecular, for having accepted me in his lab for the development of this project, for all the wise words, advices and encouragement. Thank you, for believing in me and in my abilities.

I would also like to thank all the members of the CMAzzallin lab, specially to Bruno, for always being there with his expertise and knowledgeable suggestions. Thank you for having accompanied me in this journey, with all the ups and downs that only science knows how to deliver.

An appreciation to Professor Dr. Rita Zilhão, my internal supervisor, for her availability, motivation and advices.

To my friends, thank you for all the support, for understanding that the cells have their own schedule and sometimes a coffee on the weekend is not an option.

To Ricardo, thank you for reminding me that the sun still shines outside, and that a walk by the beach helps to resolve almost everything.

Lastly, but certainly not the least, a very special thanks to my family. To my grandparents for the unconditional support, for asking "how the cells were today" even when these are concepts so hard to grasp for them. To my godmother, for all the great advices in life, for being a true role-model to follow. To my little brother, for always being there with, sometimes, not so wise words, but always full of love. To my parents, for having proportioned me the best they could and couldn't give, for always encouraging me to follow my dreams, this is only possible thanks to you both.

English Abstract

Telomeres are nucleoprotein structures located at the end of linear eukaryotic chromosomes. Telomeres have two main cellular functions, to protect chromosome ends from unwanted DNA processing and to act as a biological clock. Telomeres shorten at each cell division due to the so-called end replication problem. This progressive shortening eventually triggers replicative senescence.

Cancer cells avoid senescence by activating a mechanism that enables telomere elongation. Two different mechanism exist: re-activation of the enzyme telomerase or the Alternative Lengthening of Telomeres (ALT) pathway. ALT relies on homology-direct repair (HDR) of damaged telomeres, hence ALT telomeres need to be maintained physiologically unstable. This is achieved by endogenous replication stress accumulating at ALT telomeres. However, this DNA instability has to be kept below tolerance levels in order to avoid cell cycle arrest and death. Several factors have been identified as alleviators of telomeric replication stress in ALT cells, including the endoribonuclease RNaseH1 and the translocase FANCM.

Positive co-factor 4 (PC4) is involved in different cellular functions, including transcription, DNA replication, maintenance of genome stability and chromatin organization. Moreover, PC4 is able to bind ssDNA, dsDNA, RNA and G-quadruplexes structures, and its localization on chromatin increases upon replication stress.

This study aims at assessing if PC4 is an alleviator of ALT-specific telomeric replication stress (ATRS). I show, by indirect immunofluorescence, that PC4 localizes to telomeres and that its recruitment is enhanced when telomeric replication stress is induced through depletion of the telomeric factor TRF1. Moreover, PC4 recruitment to ALT telomeres increases upon depletion of FANCM and RNaseH1. Treatment with RNaseA shows that PC4 localization at ALT telomeres is at least in part mediated by RNA. Furthermore, expression of an ectopic PC4 mutant, W89A, shows that the capacity of PC4 to bind to ssDNA is not essential for telomere recruitment. I also show that PC4 supports ALT telomere stability since its depletion leads to accumulation of DNA damage markers at telomeres in ALT cells. This coincides with arrest of ALT cell proliferation and cell death.

This work shows that PC4 is important for ALT cell viability, likely by alleviating telomeric replication stress and avoiding excessive telomere instability. Besides uncovering a novel regulator of replication stress at ALT telomeres and further refining our understanding of ALT, this work suggests that PC4 might become an interesting target for the development of therapeutic strategies against ALT tumors.

Keywords: PC4; ALT; telomeres; replicative stress

Portuguese Abstract

As células eucariotas organizam o seu genoma em cromossomas lineares. As estruturas localizadas na porção terminal dos cromossomas são designadas por telómeros. Os telómeros são constituídos por DNA, de cadeia simples e dupla, RNA, transcrito desde a região subtelomérica, e um complexo de várias proteínas, *shelterin*. Os telómeros têm duas funções fundamentais a nível celular. Uma das funções é a de proteger a porção final dos cromossomas do processamento indesejado do DNA. Esta proteção é atingida através da aquisição de uma estrutura diferente do restante genoma. Os telómeros formam um *loop*, de forma a que a porção final do cromossoma não seja confundida com uma quebra de DNA de cadeia dupla, evitando fusões de DNA. O outro papel dos telómeros é o de operarem como o relógio biológico da célula. A cada divisão celular, os telómeros vão ficando cada vez mais curtos, devido ao *end replication problem*, isto é, a incapacidade de replicar a porção final do cromossoma. Este progressivo encurtamento dos telómeros leva à ativação de senescência replicativa, sendo considerado um mecanismo de supressão de tumores.

As células cancerígenas evitam a entrada em senescência replicativa através da ativação de um mecanismo que permite o elongamento dos telómeros. Dois mecanismos diferentes podem ser acionados: reativação do enzima telomerase; ou o mecanismo alternativo de elongamento dos telómeros (*Alternative Lengthening of Telomeres*, ALT). O enzima telomerase é fisiologicamente expresso em células germinativas, estaminais e embrionárias. Estas células, devido à sua necessidade de continua replicação, utilizam este enzima para elongar os telómeros. Cerca de 85% dos cancros exploram este mecanismo de forma a evitar senescência. Por outro lado, o mecanismo ALT, observado em aproximadamente 15% dos cancros, tem como base o mecanismo de reparação homóloga de DNA. Desta forma, os telómeros de células ALT necessitam de permanecer fisiologicamente danificados de forma a ativar o seu elongamento. Este dano é alcançado através da acumulação de *stress* replicativo nos telómeros. Contudo, esta instabilidade tem de ser mantida dentro de um determinado limite, dado que elevados níveis de *stress* despoletam morte celular. Diversos fatores foram identificados como mitigadores do *stress* replicativo em telómeros ALT, incluindo a riboendonuclease RNaseH1 e a translocase FANCM. ALT é caracterizado pela presença de vários atributos, nomeadamente: APBs, onde os telómeros se aglomeram; repetições teloméricas extra-cromossomais, como *C-circles*; troca de repetições teloméricas entre cromatídeos irmãos; mutações recorrentes do gene ATRX; elevados níveis de TERRA, o RNA transcrito dos telómeros; e telómeros heterogéneos, no que diz respeito ao seu comprimento, numa mesma célula.

O *positive co-factor* 4 (PC4) está envolvido em diversas funções celulares. Entre elas tem a capacidade de promover ou reprimir a transcrição de DNA respectivamente na presença ou ausência de um ativador, está envolvido na replicação assim como na manutenção da estabilidade genómica, atuando, por exemplo, na ativação de reparação de quebras de cadeia dupla de DNA ou na interação com p53, uma proteína supressora de tumores. PC4, mediante dimerização, é capaz de se ligar a DNA

de cadeia simples ou de cadeia dupla, a RNA e até a outras estruturas secundárias de ácidos nucleicos denominadas *G-quadruplexes*. O recrutamento de PC4 para a cromatina é amplificado após a indução de *stress* replicativo.

Este estudo pretende avaliar o papel de PC4 enquanto um mitigador de *stress* replicativo específico de telómeros ALT. Eu demonstro, através de imunofluorescência, que apenas uma porção de PC4 se encontra acoplado à cromatina. Deste PC4 algum localiza-se nos telómeros. O recrutamento de PC4 é estimulado através da indução de *stress* replicativo especificamente nos telómeros através da depleção de TRF1, um fator telomérico. Adicionalmente, um maior recrutamento de PC4 para os telómeros ALT é observado aquando da depleção de FANCM, RPA70 e RNaseH1, conhecidos aliviadores de *stress* replicativo específico de telómeros ALT. O tratamento com RNaseA evidencia que a localização e manutenção de PC4 nos telómeros ALT é pelo menos em parte dependente de RNA. A expressão ectópica de um mutante de PC4 (W89A), que não possui capacidade de se ligar a DNA de cadeia simples, demonstra que esta capacidade de PC4 não é necessária para o seu recrutamento para os telómeros. Eu também demonstro, com o presente estudo, que PC4 suporta a estabilidade dos telómeros ALT. A depleção de PC4 leva a acumulação de marcadores de dano genómico específico de telómeros de células ALT. No entanto, não se observa uma alteração nos níveis de *shelterin*, não sendo, portanto, esta a causa da instabilidade telomérica. Esta instabilidade telomérica, após a depleção de PC4, resulta numa perda da capacidade proliferativa e morte das células ALT, observada através da realização de curvas de crescimento. Este estudo excluí a hipótese de ativação de apoptose após depleção de PC4, contudo é levantada a hipótese de uma possível ativação de autofagia.

Este trabalho demonstra que PC4 é importante para a viabilidade das células ALT. Possivelmente, PC4 atua como aliviador de *stress* replicativo telomérico, evitando excessiva instabilidade nestas estruturas. Para além de revelar um novo regulador de *stress* replicativo nos telómeros ALT, e aprimorar o nosso conhecimento do mecanismo ALT, este trabalho sugere que PC4 poderá ser um candidato interessante no que diz respeito à abordagem terapêutica de cancros ALT.

Palavras chave: ALT; PC4; telómeros; *stress* replicativo

Index

List of figures

List of tables

List of abbreviations

ALT: alternative lengthening of telomeres

APBs: ALT-associated PML bodies

ATRS: ALT-specific telomeric replication stress

ATRX: alpha thalassemia/mental retardation syndrome X-linked gene

BIR: break-induced replication

BTR: BLM/TOP3A/RMI1/2 complex

CkII: casein kinase II

CTD: C-terminal domain

DDR: DNA damage response

DSB: double-stranded break

DSBR: double-stranded break repair

dsDNA: double-stranded DNA

ECTRs: extrachromosomal telomeric repeats

EMSA: electrophoretic mobility shift assay

FANCM: Fanconi anemia complementation group M

G4s: G-quadruplexes

HDR: homology-direct repair

HR: homologous recombination

HU: hydroxyurea

IF: immunofluorescence

K-rich: lysine-rich

LC3B: microtubule-associated protein 1 light chain 3

lncRNA: long noncoding RNA

NHEJ: non-homologous end joining

OB: oligonucleotide/oligosaccharide binding

PARP: poly(ADP-ribose) polymerase

PC4: positive co-factor 4

PCNA: proliferating cell nuclear antigen

PE: phosphatidylethanolamine

PIC: preinitiation complex

PML: promyelocytic leukemia protein

POT1: protection of telomeres 1

P-PC4: phosphorylated PC4

pSer33: RPA32 phosphorylated at serine 33

RAP1: repressor-activator protein 1

RBP: RNA binding protein

RFC: replication factor C

RNAPII: RNA polymerase II

RNAPIII: RNA polymerase III

RPA: replication protein A

RRM: RNA recognition motifs

SEAC: serine and acidic residue-rich domain

ssDBD: ssDNA binding domain

ssDNA: single-stranded DNA

SV40: simian virus 40

TAFs: TBP-associated factors

TALEs: transcription activator-like effectors

TBP: TATA-binding protein

telR-loop: telomeric R-loop

TERRA: long non-coding telomeric RNA

TERT: Telomerase catalytic component

TIN2: TRF1-interacting nuclear protein 2

T-loop: telomeric loop

TMM: telomere maintenance mechanism

TPP1: TIN2 and POT1-interacting protein

TRF1: telomeric repeat binding factor 1

TRF2: telomeric repeat binding factor 2

T-SCE: telomeric sister chromatid exchange

WB: western blotting

γH2AX: histone H2A variant phosphorylated at serine 139

1. Introduction

1.1 Telomeres: Structure and function

Prokaryotic and eukaryotic cells have distinct ways of organizing their genome. Prokaryotic cells usually organize their genome in a unique single circular chromosome. Conversely, in the large majority of eukaryotic cells, the genetic information is comprised within linear chromosomes. At the ends of these chromosomes there are structures called telomeres. The word telomere derives from two Greek words, *telo* meaning "end" and *meros* meaning "part".

The presence of a stabilizing structure at the end of chromosomes was firstly suggested by Hermann Muller, in 1938, and Barbara McClintock, in 1941, in independent studies (1,2). However, the available tools at the time hindered further characterization. Only in 1978, the molecular composition of telomeres was described by Elizabeth Blackburn and Joe Gall in *Tetrahymena termophila* (3). Posterior studies, in budding yeast, executed by Blackburn in collaboration with Jack Szostak, revealed that telomeres are functionally conserved throughout phylogenic kingdoms (4). Robert Moyzis *et al* later reported that human telomeres comprise tandem repeats of TTAGGG (from 5' to 3' end), hence being composed by a G-rich and a C-rich strand (5). Since then, telomeres have been intensively studied and defined as evolutionary well-conversed sequences, (6) with two main purposes in the cell i) to act as biological clocks (7,8) and ii) to protect chromosomes against end-to-end fusion and erosion (9). The discovery of "how chromosomes are protected by telomeres" by Blackburn and Szostak was rewarded in 2009 with the Nobel Prize in Physiology or Medicine (prize also shared with Carol Greider).

Telomeres are comprised of telomeric double-stranded DNA (dsDNA) as well as telomeric single-stranded DNA (ssDNA), the latter corresponding to a G-overhang or G-tail (Figure 1.1). The G-tail arises from resection of the C-rich strand from 5' to 3' and is composed of 75-200 bases of DNA in humans (10). The repetitive nature of telomeric DNA allows the intramolecular pairing of the 3' overhang with the C-rich strand. This leads to the formation of a D-loop, due to the displacement of the G-rich strand through the invasion of the G-tail into the telomeric dsDNA, and an overall lasso-like structure called T-loop, (Figure 1.1) (11). The T-loop, being a structure different from the rest of the genome, allows the DNA repair machinery to distinguish between the end of a chromosome and a DNA double-stranded break (DSB). Hence, the telomere acts as a chromosome cap that avoids DNA damage response (DDR) activation and non-homologous end joining (NHEJ) (12).

Shelterin, a nucleoprotein complex that associates with human telomeres, is composed in humans of six different proteins: TRF1, TRF2, TIN2, RAP1, POT1 and TPP1 (Figure 1.1). TRF1 (telomeric repeat binding factor 1) and TRF2 (telomeric repeat binding factor 2) recognize and bind with high affinity to (5'-TAGGGTT-3')n dsDNA through their C-terminal Myb domains upon homodimerization mediated by their TRFH domain (13–15). *In vitro* and *in vivo* assays demonstrated that TRF2 is necessary and sufficient for the formation of T-loops (16,17). TIN2 (TRF1-interacting nuclear protein 2) links TRF1 and TRF2 through protein/protein interactions (18). RAP1 (repressor-

activator protein 1 homolog) binds to TRF2 (19). POT1 (protection of telomeres 1) binds to ssDNA by its oligonucleotide/oligosaccharide binding (OB) folds, OB1 and OB2 domains (20). TPP1 (TIN2 and POT1-interacting protein), as the name indicates, interacts with TIN2 and POT1 (21).

Shelterin supports various functions, including the formation of the G-rich overhang (22) and consequent formation of T-loops (23). Shelterin is also involved in the repression of ataxia-telangiectasia-mutated (ATM) signaling. It also plays a role in chromosome protection by shielding the G-overhang against DSB repair (DSBR) through repression of NHEJ (21,24).

Telomeres are transcribed into the long non-coding RNA (lncRNA) TERRA by RNA polymerase II (RNAPII) (25,26). Transcription of telomeres starts from the subtelomeric region and uses the C-rich telomeric strand as a template; hence TERRA comprises telomeric UUAGGG repeats (Figure 1.1). TERRA promoters have been identified on approximately half of human subtelomeres. They comprise CpG dinucleotide-rich tandem repeats of 29 and 37 base pair, and methylation of these CpG promoter islands negatively regulates TERRA transcription (27). However, TERRA transcribed from other chromosome ends has been detected, indicating the existence of different promoters still to be identified (28). TERRA molecules remain in the nucleus after transcription, localizing mainly to telomeres (25). TERRA can anneal with telomeric DNA forming RNA:DNA hybrids named telomeric R-loops (telR-loops) (Figure 1.1). TERRA is associated with a large number of telomeric functions including regulation of telomere length, promotion of DNA-end processing and enabling telomere protein composition changes (25,26).

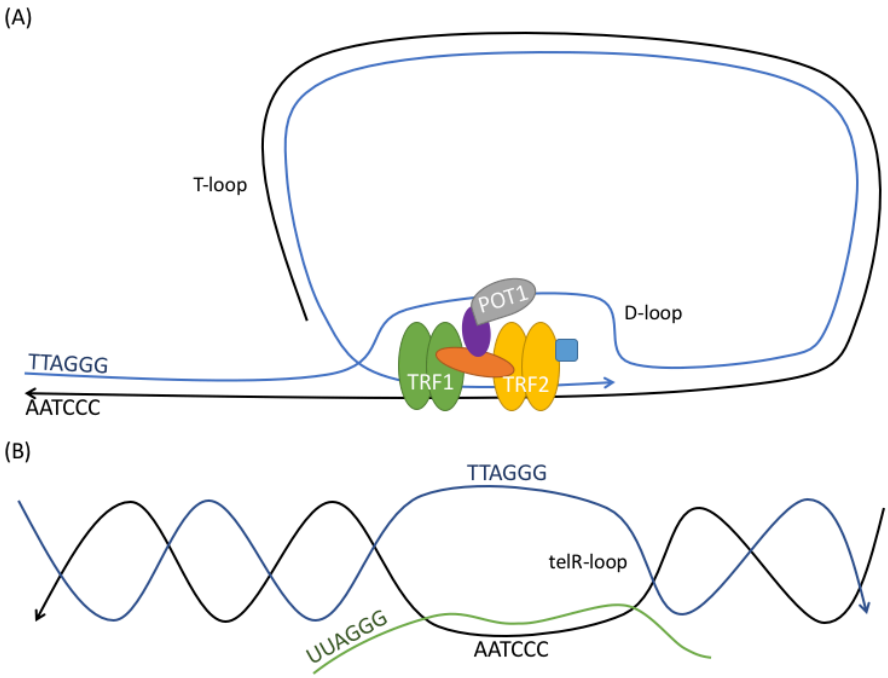

Figure 1.1 Telomeric structure. (A) Depiction of telomeric loop (T-loop), and D-loop, formed through G-overhang (blue strand) invasion of telomeric dsDNA. Strand arrows represent DNA directionality from 5' to 3'. Shelterin components are pictured, TRF1 (green), TRF2 (yellow), TIN2 (orange), TPP1 (purple), RAP1 (blue) and POT1 (grey); (B) Representation of telomeric R-loop (telR-loop), TERRA (green) invading telomeric DNA and annealing with C-rich telomeric strand.

Telomeres are regions of the chromatin with high levels of replication stress. This is due to formation of secondary structures at telomeres (29), such as telR-loops, T-loops, D-loops and G-quadruplexes (G4s). G4s structures are very abundant at telomeres due to their G-rich nature. Guanines assemble in tetrameric structures, forming stacked G-quartets (square planar arrangements in which each guanine is hydrogen bounded to the two adjacent guanines) (30).

In 1961, Leonard Hayflick uncovered for the first time that primary human cells are not immortal, and that they can undergo only a certain number of divisions before experiencing cell cycle arrest. Hayflick termed senescence as the progressive and irreversible loss of proliferative potential of somatic cells (7). This suggests the presence of an internal counting mechanism within the cell (7). Later in 1972, Alexey Olovnikov linked this mechanism to the end of the chromosomes (8). Canonical DNA polymerases are unable to fully replicate the end of a linear chromosome through lagging strand synthesis, a notion that is known as the end replication problem (31). Hence, as each replication goes by, telomeres get shorter, losing around 200 bp per replication round in humans. When an aging cell accumulates telomeres that are too short, below a certain threshold, it enters replicative senescence through the activation of the tumor suppressor protein p53 (32).

Normal human somatic cells do not have mechanisms to elongate telomeres (31). This absence allows the cell to have a cellular clock limiting proliferation and contributing to the aging process (7,31). Embryonic, germline and stem cells, on the other hand, need to replicate many more times than somatic cells (33). To avoid senescence, these cells possess a mechanism that allows telomeres to elongate. In order to perform that, germline cells express a reverse transcriptase telomerase, which avoids telomere shortening and consequently senescence (33).

Telomerase, discovered by Blackburn and Carol Greider in 1985, is a nucleoprotein complex capable of elongating telomeres (34). Human telomerase is composed of two major components, hTR and TERT. Both components form a complex that is sufficient for the novel synthesis of telomeric repeats. Telomerase catalytic component (TERT) acts by adding newly synthesized telomeric repeats to the end of chromosomes, using a RNA template (hTR) (35). Telomere elongation coincides with the time of telomere replication (36), however, not all telomeres are elongated in the same cell cycle but only the shortest ones in the cell (37).

1.2 ALT

One of the hallmarks of cancer is the enabling of replicative immortality, which can be achieved by activating a telomere maintenance mechanism (TMM) (38). Approximately 85% of the cancers re-activate the expression of telomerase (39), while 15% engage the Alternative Lengthening of Telomeres (ALT) mechanism (40). ALT tumors are mainly of mesenchymal or neuroepithelial origin, including osteosarcomas, liposarcomas, astrocytomas and glioblastomas (41).

ALT cells are characterized by different molecular features, including ALT-associated ProMyelocytic Leukemia (PML) bodies (APBs) and extrachromosomal telomeric repeats (ECTRs).

APBs are structures where telomeric DNA clusters together with TERRA, shelterin components and DNA recombination and repair factors (42–44). ECTRs can be of circular or linear nature, comprising double-stranded (ds) circles (t-circles), partially single-stranded (ss) circles (either G-circles or C-circles) and linear dsDNA (45,46). The telomeres of ALT cells are very heterogenous in length, having the same cell very long telomeres, in comparison to the average length of telomeres in telomerase-positive cells, as well as very short telomeres (40). Other frequent features of ALT cells are exchange of telomeric DNA between sister chromatids (T-SCE) (47), recurrent mutations of the Alpha Thalassemia/Mental Retardation Syndrome X-Linked (ATRX) gene (48) and high levels of TERRA (and consequent increased levels of telR-loops) due to TERRA promoter hypomethylation (25,49–51).

Telomere elongation in ALT occurs in the G2/M phases of the cell cycle by homology-directed repair (HDR) through break-induced replication (BIR) (52). BIR is a conservative type of DNA synthesis used for the repair of one-ended DSBs (52). ALT BIR was firstly identified in budding yeast survivors after crisis mediated by telomerase inactivation (53). Two different types of survivors were described, type I and type II (54,55). ALT type I and II rely both on Rad52 and Pol32, however type I also requires Rad51 (53,54,56).

ALT, in human cells, relies on replication factor C (RFC), proliferating cell nuclear antigen (PCNA) and the DNA polymerase δ accessory subunits POLD3 and POLD4 (57–59). APBs are believed to be the site where BIR occurs, by bringing telomeres together and promoting telomere-telomere interactions (43). ALT telomeres, with elevated levels of DNA damage, are brough together in a BLM-mediated manner at APBs (58,60) and this is counterbalanced by SLX4 (61). PML is required for the ALT mechanism (58), having a role in the recruitment of the BLM/TOP3A/RMI1/2 (BTR) complex to telomeres (60). This is followed by a bifurcated ALT pathway with a branch RAD52-dependent and another one RAD52-independent (58,62). The first branch, RAD52-dependent, is important for maintenance of ALT telomeres through telomeric DNA synthesis in APBs (62). The other branch, RAD52-independent, besides elongating telomeres, is responsible for C-circle formation (58). Upon replication fork collapse, if fork regression does not occur, the cell produces C-circles as a mean to avoid high levels of telomere instability (63). Furthermore, depletion of RAD51, which is not necessary for maintenance of ALT telomeres in the RAD52-dependent pathway, has a role in suppressing C-circle formation in the RAD52-independent branch (58). For BIR to occur it is necessary to have annealing of telomeric ssDNA with a template for the synthesis of new telomeric DNA (40,64). The template can be the telomere itself, a telomere on a sister chromatid or on another chromosome (40,64). RAD52 has the capability to anneal telomeric ssDNA in the presence of replication protein A (RPA), which is known to be present at APBs (50,65) and to promote the invasion of telomeric ssDNA into telomeric dsDNA (58).

ALT cells, when compared with telomerase-positive and primary cells, have more abundant replication stress and DNA damage markers at telomeres (66–68). This arises from the necessity of ALT cells to maintain at least a subset of telomeres physiologically damaged for telomere elongation to occur.

The annealing of TERRA with telomeric DNA, telR-loops, more abundant in ALT than telomerase-positive cells, are one of the triggers of this ALT-specific Telomeric Replication Stress (ATRS) (50). If replication stress is excessive, DNA damage checkpoints will be activated and impair cell proliferation or induce cell death (51,67). In order to keep telomere elongation and avoid cell cycle arrest and death, ALT cells need to have constantly active alleviators of ATRS (50,51). Thus, a balance between alleviators and triggers of ATRS must be maintained in ALT cells.

A known alleviator of ATRS is RNaseH1, a RNA endonuclease that is enriched at ALT telomeres and restricts the levels of telR-loops (50). Its depletion leads to increased ATRS through the increase of telR-loops, telomere loss and exposure of telomeric ssDNA (50). In contrast, overexpression of RNaseH1 leads to telomere shortening due to declining of ATRS and recombinogenic potential (50).

Fanconi anemia complementation group M (FANCM) is another known ATRS alleviator (51,69,70). FANCM depleted ALT cells have massive telomere disfunction, as shown by accumulation of DNA damage markers at telomeres (51). The presence of ALT features is highly increased upon depletion of FANCM (51). FANCM-depleted cells also accumulate telR-loops and ultimately die (51). Besides RNaseH1 and FANCM, other ATRS alleviators have been described including SMARCAL1 (71) and ATR (65).

1.3 PC4

Positive co-factor 4 (PC4) was first identified in 1994 by Ge and Roeder (72). Since then, PC4 has been identified both in prokaryotes and eukaryotes indicating that it is an evolutionary conserved protein (73–75). It was firstly described as a non-essential activator of basal transcription (72), however it is now clear that PC4 is involved in many cellular functions that go beyond transcription regulation.

PC4 is a protein constituted by 127 amino acids. It possesses, at its N-terminus (residues 1-62), a lysine-rich (K-rich) domain flanked by two serine and acidic residue-rich (SEAC) domains (Figure 1.2) (72). PC4 N-terminus is responsible for binding to dsDNA in a sequence-independent manner (76) and for interaction with transcriptional co-activators (77–79). The C-terminal region (residues 63-127) contains a ssDNA binding domain (ssDBD) (72,80). PC4 is also capable of binding melted dsDNA originating from the localized dissociation of dsDNA helix into single strands. Both opposing ssDNA regions are necessary for binding with PC4, with a maximum of 8 nucleotide mismatches, while it needs 16 to 20 nucleotides to fully bind to ssDNA (76,80). It has been demonstrated that PC4 is a DNA bending protein, explaining the requirement for more free nucleotides for the interaction with a fully ssDNA (81). PC4 also holds the capacity to bind to G4s *in vitro*, without destabilizing them, in a manner distinct from the way it interacts with ssDNA (82,83). PC4 capacity to bind to RNA was also suggested (84) and is further supported by the similarities between the C-terminal domain (CTD) of PC4 and RNA recognition motifs (RRM) of RNA-binding proteins (RBPs) (75,85).

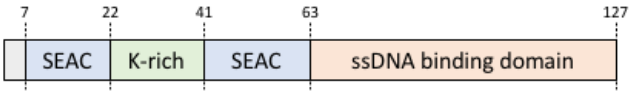

Figure 1.2 Schematic representation of PC4 and its structural and functional domains. N-terminal region of PC4, residues 1-62, contains two serine and acidic residue-rich domains (SEAC, blue) flanking a lysine-rich domain (K-rich, green). C-terminal region, residues 63-127, contains a ssDNA binding domain (orange).

PC4 3D structure, solved by crystallography, reveals a complex in which two monomers dimerize through a dimerization domain present in the C-terminal region (86,87) (Figure 1.3). Each monomer is comprised of a curved four-stranded anti-parallel β-sheet followed by a kinked α-helix (β-β-β-β-α), in a domain-swapped manner, with the α-helices packed against the β-sheets of their dimeric partner (86,87). PC4 dimers present a β-ridge (residues 87-101) formed by the extension of the aligned strands β3 and β4 (86). Quarter pipe structures (or concave β-surfaces) with opposite directionality and divided by the β-ridge are formed by a β2-β3 loop (86).

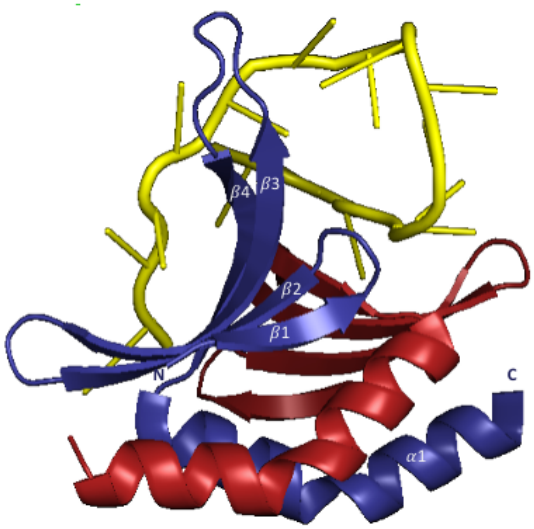

Figure 1.3 Crystal structure of PC4. Crystal structure of PC4 ssDNA-binding domain homodimer (red and blue) in complex with a ssDNA oligonucleotide (yellow). Figured prepared by PyMol from PDB ID code 2C62(87).

Werten *et al*. demonstrated the importance of the β2-β3 loop and the β-ridge for the interaction with ssDNA and melted dsDNA, through the mutation of an aromatic residue (Phe77) in the β2-β3 loop as well as the replacement of Trp89 in the β-ridge by Ala89 (W89A) (77,88). Conversely, Phe77 mutation did not abolish the ability of PC4 to bind to RNA (84). PC4 dimers interact with melted heteroduplexes by binding of pseudo symmetrical opposing regions with the quarter pipes, with ssDNA-hairpin enfolded around the β-ridge. This conformation, with the ssDNA backbone tethered to PC4 by water molecules, leaves the DNA bases facing outwards and able to bind in a specific manner to other biomolecules (87). Both PC4 subunits of the dimer are needed for ssDNA binding and cooperate in the binding of the two opposing DNA backbones (87).

PC4 was initially described as not essential for basal transcription, but in cooperation with TATA-binding protein (TBP)-associated factors (TAFs) mediates transcriptional activation of RNA

polymerase II (72). Further studies showed a dual role for PC4 in transcription initiation. In TAFs absence, PC4 strongly represses transcription initiation, inhibiting transcription prior to preinitiation complex (PIC) assembly (79,89). PC4 ability to bind to melted DNA is required for transcription repression (77) and this repression is alleviated by the helicase activity of TFIIH (78). In the presence of an activator or already assembled PIC, PC4 acts as a coactivator, mediating transcriptional activation (79). The N-terminal domain of PC4 is essential for this activator role (79).

PC4 activity is negatively regulated by phosphorylation. Ninety-five percent of PC4 found in HeLa cell extracts is phosphorylated (P-PC4) (90). Phosphorylation of PC4 is executed by casein kinase II (CkII), being restricted to seven residues of the N-terminal portion (90,91). P-PC4 has a stronger ssDNA binding capacity than PC4, conversely P-PC4 loses the potential to activate transcription and binds less strongly to RNA (84,86,90,91). PC4 N-terminus can also be acetylated by p300, however P-PC4 cannot be acetylated as phosphorylation could impose a structural change in PC4 masking the acetylation sites (92). Acetylation of PC4 leads to an increase of DNA bending activity (81).

PC4 functions in transcription are not only restricted to activation or inhibition. Interaction of PC4 with the polyadenylation factor CstF-64 prevents premature transcription termination by RNAPII (93). A role in accurate termination and multiple-round transcription by RNA polymerase III was also described (94). PC4 can also stimulate promoter escape in the presence of transcriptional activators, such as GAL4-VP16 (95).

Pan *et al*, in 1996, demonstrated that PC4 could have a role in DNA replication, by either inhibiting or activating, in a concentration dependent manner, simian virus 40 (SV40) DNA replication. SV40 needs RPA for DNA unwinding in order to be replicated and PC4 forms complexes with RPA on ssDNA, leading to a modulation of RPA replication functions (96). Further studies reported that RPA and PC4 bind to ssDNA in a similar manner (77). Successive studies supported this notion by showing an increased loading of PC4 to ssDNA upon RPA depletion (97).

PC4 is also involved in maintenance of genome stability. PC4 is stably associated with chromatin through all cell cycle. It interacts directly with H3 and H2B, being able to regulate chromatin folding, such as transition from transcriptionally silent heterochromatin to more-open transcriptionally active euchromatin (and vice-versa) (98,99). Knockdown of PC4 in HeLa cells, led to decondensing of chromatin and consequent over-expression of several genes (98).

PC4 has an important role in resistance to hydrogen peroxide and in the repair of mutations of spontaneous or oxidative damage nature, mediated by its interaction with XPG, a DNA repair protein (100). The W89A mutant does not possess the ability to prevent spontaneous and induced oxidative mutagenesis. PC4 role in DNA damage repair is supported by the demonstration that it accumulates at DNA damage sites, like replication-transcription collision sites, in a fast and transient manner and dependent on its ssDNA-binding activity (97,101). Additionally, it was shown that PC4 is involved in DNA damage repair by NHEJ and homologous recombination (HR) (101,102), with residues 72-77 of PC4 responsible for this function and transcriptional coactivation ability not being required (102).

PC4 can also interact with p53 *in vivo* and enhances DNA binding activity of p53 *in vitro* (81,103). PC4 interacts with p53 through its ssDNA binding domain and thus ssDNA and p53 compete for the same binding site on PC4 (81,104). Post-translational alterations of PC4 can modulate the activation of p53 (81). Phosphorylation of PC4 abolishes interaction with p53, while acetylation of PC4 enhances the DNA binding capacity of p53 due to PC4-induced alteration in DNA conformation (81).

Recent studies have reported upregulation of PC4 in different tumors, including astrocytoma (105), osteosarcoma (106), non-small cell lung cancer (107) and breast cancer (108) and its association with cancer progression and decreased survival. Elevated expression of PC4 in breast cancer was described to positively correlate with metastasis and poor prognosis of patients, through the regulation of c-Myc transcription (108). Zhang *et al*. reinforced these notion by showing that predicted targets of PC4 were up-regulated in many cancer types (109).

2. Objectives

ALT cells need to keep a tight balance between triggers and alleviators of ATRS in order to maintain replication stress at telomeres within tolerable levels. Triggers of ATRS are necessary to keep telomere elongation and avoid senescence. However, high levels of ATRS will lead to impaired proliferation and/or cell death, hence the importance of alleviators.

PC4 recruitment to chromatin is enhanced upon replication stress, leading us to hypothesize that PC4 might be one ATRS alleviator in ALT cells. In order to test this hypothesis, this project has the following specific aims:

1. Understand if PC4 localizes to telomeres, and if so, why and how it is recruited;
2. Understand if PC4 depletion affects telomere integrity in ALT cells by evaluation of DNA damage markers at telomeres;
3. Test if loss of PC4 affects ALT cells survival and growth.

This study has the purpose to further clarify the mechanisms underlying ALT. The acquisition of new knowledge in this field can potentially lead to new therapeutic targets in ALT cancers.

3. Methods

3.1 Cell lines and culture conditions

HeLa (human cervix carcinoma) and HEK293 (human embryonic kidney) cells were obtained from ATCC. U2OS (osteosarcoma cells) were generously offered by M. Lopes (IMCR, Zurich, Switzerland) and Saos-2 and HOS (osteosarcoma cells) were a kind gift from B. Fuchs (Balgrist University Hospital, Zurich, Switzerland).

HeLa and U2OS were cultured in high glucose DMEM, GlutaMAX (Thermo Fisher Scientific) supplemented with 100 U/ml of penicillin-streptomycin (Thermo Fisher Scientific) and 5% tetracycline-free fetal bovine serum (Pan BioTech). Saos-2 and HOS were maintained in high glucose DMEM/F12,

GlutaMAX (Thermo Fisher Scientific) supplemented with 100 U/ml of penicillin-streptomycin (Thermo Fisher Scientific), 10% tetracycline-free fetal bovine serum (Pan BioTech) and 5% of non-essential amino acids (Thermo Fisher Scientific). When mentioned, cells were incubated with 2 mM of hydroxyurea (HU) (Sigma-Aldrich) for 24 h and 1 μM of camptothecin (CPT) (Sigma-Aldrich) for 3 h. All cells were grown in a humidified atmosphere at 37 °C containing 5% CO_2.

3.2 siRNA-mediated protein depletion

DsiRNAs (Integrated DNA Technologies) were transfected using the Lipofectamine RNAiMAX reagent (Invitrogen) according to the manufacturer's instructions. Briefly, DsiRNAs and Lipofectamine were separately diluted in Opti-MEM (Thermo Fisher Scientific) and the two solutions were mixed and incubated at room temperature (RT) for 5 minutes. This mixture was then further diluted 1:5 in growth medium and applied to the cells. DsiRNAs for FANCM, RPA70, RNaseH1 and TRF1 were used at a final concentration of 20 nM, while DsiRNAs for PC4 were used at a final concentration of 30 nM (unless otherwise indicated). Medium was changed 5h after transfection. Samples were collected after 48 h, for FANCM, RPA70, RNaseH1 and TRF1 depletion, and 72h, for PC4 depletion, after transfection (unless otherwise indicated). The mRNA target sequences used can be found in annex Table 7.1.

3.3 Expression of ectopic proteins

For PC4 WT complementation experiment, Saos-2 cells were infected twice with retrovirus produced using the pBABEneo-Flag-PC4 plasmid, followed by selection in medium containing 1 mg/mL of G418. The pBABEneo-Flag-PC4 plasmid contained an siRNA-resistant human wild-type PC4 tagged at the N-terminus with two Flag epitopes, under the control of LTR promoter. PC4 WT ectopic protein expression was confirmed by western blotting.

For PC4 WT and W89A experiments, U2OS cells were infected twice with retroviruses produced using the pLHCX-Flag-PC4 and pLHCX-Flag-PC4-W89A plasmids, followed by selection in medium with 200 μg/ml hygromycin B (VWR). pLHCX-Flag-PC4 and pLHCX-Flag-PC4-W89A plasmids contained an siRNA-resistant human wild-type or W89A PC4 2xFlag-tagged, under the control of CMV promoter. PC4 WT and W89A ectopic proteins expression were confirmed by western blotting.

Viruses were produced in HEK293 cells according to standard procedures. Briefly, HEK293 seeded in 6 cm dishes were transfected, using Lipofectamine 2000 (Invitrogen), with 2000 ng of transgene plasmid and 500 ng pMD-VSVG (VSV-G plasmid) and 1500 ng pMDGAG/POL (Gag-Pol plasmid) packaging plasmids, in a total culture medium volume of 2,5 ml. Fourteen and twenty-two hours post transfection medium was discarded and replaced with fresh medium. Forty-eight hours post transfection medium was recovered and filtered using 0,45 μm syringe filters, diluted 1:2 with fresh warm medium, and dispensed on target cells (U2OS and Saos-2) previously seeded. Twenty-four hours later, a second infection was performed followed by selection 24 h later.

3.4 Cell proliferation assays

For growth curves, cells were transfected with siRNAs (day 0) and 24 h later seeded in 6 cm dishes in triplicates (75000 HeLa, 150000 Saos-2, 100000 U2OS and HOS) (day1). DsiRNAs were re-transfected at day 3 and cells were counted and seeded again 24 h later (day 4). Cells were re-transfected and counted every 3 days. Cells were counted under the microscope using a Neubauer chamber.

3.5 Western blotting

Cells were trypsinized and pelleted by centrifugation at 500 x g at 4 ºC for 5 min. Pellets were washed twice in 1x PBS and resuspended in 2x Laemmli buffer (4% SDS, 20% Glycerol, 120mM TrisHCl pH 6,8). Samples were homogenized by syringing and denatured at 95ºC for 5 min. Protein concentrations were determined using a Nanodrop 2000. Fifteen to thirty micrograms of protein extracts were supplemented with 0.005% Bromophenol blue and 1% β-Mercaptoethanol (Sigma-Aldrich), incubated at 95 °C for 5 min, separated in 6, 8, 10 or 14% polyacrylamide gels, and transferred to nitrocellulose membranes (Maine Manufacturing, LLC) using a Trans-Blot SD Semi-Dry Transfer Cell apparatus (Bio-Rad). Membranes were counterstained with Ponceau, and protein blocking was performed by incubating the membranes in 5% skim-milk in 1x PBST (0,1% Tween-20 in 1x PBS). Primary antibodies were diluted in blocking solution and incubated with the membrane for 1 h at room temperature (RT) or overnight at 4 ºC. Membranes were washed three times in 1x PBST with gentle shaking and then incubated with secondary antibodies HRP-conjugated for 1 h at RT. The antibodies used are listed in annex Table 7.2. Signal detection was performed incubating the membranes with an ECL detection reagent (GE Healthcare) followed by acquisition using an Amersham 680 RGB imaging apparatus (GE Healthcare).

3.6 Indirect Immunofluorescence (IF)

Cells were grown on coverslips and, unless otherwise mentioned, soluble proteins were pre-extracted by incubation in buffer CSK (0,5% Triton X-100, 10 mM PIPES pH 7, 100 mM NaCl, 3 mM MgCl2, 300 mM Sucrose) for 7 min on ice. The subsequent treatments were performed at RT. When mentioned, cells were treated with 200 µg/ml of RNaseA (Nzytech) in 1x PBS for 10 min. Cells were fixed in 3,6% formaldehyde (Sigma-Aldrich) in 1x PBS for 10 min, permeabilized with CSK buffer for 7 min and incubated in blocking solution (0,5% BSA, 0,1% Tween-20 in 1xPBS) for 45 min. Coverslips were incubated with primary antibodies diluted in blocking solution for 1 h in a humid chamber, washed three times with 0,1% Tween-20 in 1x PBS for 10 min each, incubated with blocking solution containing secondary antibodies for 40 min, washed three times with 1x PBST for 10 min each and washed once with PBS for 10 min. DNA was counterstained with 100 ng/ml DAPI in 1x PBS. Coverslips were mounted on slides with Vectashield. Images were acquired with a Zeiss Cell Observer equipped with a cooled Axiocam 506m camera and a x63/ 1.4NA oil DIC M27 PlanApo N objective. Image analysis was performed using ImageJ. Primary and secondary antibodies used are listed in annex Table 7.3.

3.7 RNA extraction

Total RNA was extracted with the NucleoSpin RNA Kit from Macherey-Nagel. Cells were harvested by scraping and lysed in 350 µl of RA1 buffer (Macherey-Nagel) supplemented with 1% β-Mercaptoethanol. Lysates were filtered by centrifugation at 11000 g for 1 min through a NucleoSpsin Filter. RNA binding conditions were adjusted by addition of 350 µl of 70% Ethanol. RNA was bound to a NucleoSpin RNA Column through centrifugation at 11000 g for 30 sec. The silica membrane was desalted with addition of 350 µl of Membrane Desalting Buffer and centrifugation at 11000 g for 1 min. DNA digestion was performed on column at RT for 15 min with 1:10 dilution of reconstituted rDNase in Reaction Buffer. The silica membrane was washed first with RAW2 and then twice with Buffer RA3. RNA was eluted in 40 µl of RNase-free H_2O by centrifugation at 11000 g for 1 min. RNA was stored at -80 ºC.

3.8 cDNA synthesis

RNA concentrations were determined using a Nanodrop 2000. cDNA synthesis was performed with SuperScript II RT (Invitrogen) in a reaction volume of 20 µl in a Biometra TRIO Thermal Cycler Series (Analytik Jena). One microgram of total RNA was used together with 1 µl of Oligo(dT) at 500 µg/ml, 1 µl of 10 mM dNTP Mix (Invitrogen) and nuclease-free water up to 13 µl. The mix was heated to 65 ºC for 5 min and quickly chilled on ice. Four microliters of 5x First-Strand Buffer (Invitrogen) and 2 µl of 0,1 M DTT (Sigma-Aldrich) were added to the mix, followed by incubation at 42 ºC for 2 min. One microliter of SuperScript II RT was added to the mix, mixed by gently pipetting up and down. Incubation was performed at 42 ºC for 50 min, followed by inactivation of the reaction by heating at 70 ºC for 15 min. For each sample, a negative control was performed by adding nuclease-free water to the reaction instead of SuperScript II RT. The total reaction volume of 20 µl was diluted 5-fold with RNase-free water before use.

3.9 RT-qPCR

Reverse transcription quantitative PCR (RT-qPCR) was performed by amplification of 2 µl of diluted cDNA in a mix containing 6 µl of RNase-free water, 1 µl of 10 µM of each primer, forward and reverse (in annex Table 7.4), and 10 µl of iTaq Universal SYBR Green Supermix (Bio-Rad). Each sample was amplified in triplicate, while control samples for cDNA synthesis (without SuperScript II RT) were amplified only once. One negative control without template was also used in each run for each primer mix used. The amplification was carried in a Rotor Gene Q instrument (Qiagen) with the following settings: 5 min at 95 ºC followed by 45 cycles of 15 sec at 95 ºC (denaturation) and 30 sec at 60 ºC (annealing and amplification). A melting step was performed by gradually rising temperature by 1 ºC each step, from 50 to 99 ºC. The acquisition was performed using the green channel with a gain value of 9. Results were analyzed using Rotor Gene 6000 Series software. U6 was used as a normalizer.

3.10 Statistical Analysis

To directly compare two different groups, a non-parametric two-tailed Mann-Whitney U test was employed using GraphPad Prism. P values are indicated as: *P<0,05; **P<0,005; ***P<0,001; ****P<0,0001.

4. Results and Discussion

4.1 PC4 localizes to telomeres

Previous studies have suggested that PC4 could be a component of telomeres; indeed PC4 was identified in mass spectrometry-based large-scale screenings for TERRA and telomeric DNA interacting proteins (110,111). Given that increased PC4 recruitment to chromatin has been shown upon treatment with replication stress-inducing agents (101), and since telomeres are regions prone to replicative stress in particular in ALT cells (51), we tested if PC4 could be detected at telomeres by indirect immunofluorescence (IF).

In order to validate the specificity of our antibody against PC4, I knocked-down PC4 in U2OS cells and performed western blotting (WB) for PC4. PC4 depletion was tested by transfecting ALT U2OS cells with 3 different siRNAs (siPC4a, siPC4b and siPC4c) at 20 nM concentrations for 72 h. An siRNA (siCt) that does not target any human genes was used as a negative control. WB was performed using total protein extracts to confirm protein depletion and PC4 signals were normalized to the ones detected with an antibody against β-Actin. As shown in Figure 4.1A, depletion was efficient after transfection with both siPC4b and siPC4c, with more than 90% of endogenous PC4 being depleted. On the other hand, in cells transfected with siPC4a, 32% of protein remained. The concentration of siRNAs was then increased to 30 nM to optimize depletion. Indeed, the depletion of PC4 was further improved, being siPC4b more efficient than siPC4c, with 97% depletion and 94% depletion, respectively. It was also possible to conclude that the antibody is highly specific when used in WB, given the absence of other bands besides the expected band size for PC4 (~15kDa) (Figure 4.1A).

After optimizing the transfection conditions, an IF was performed with siRNA-transfected cells (30 nM concentration) using conditions allowing detection of total proteins (no pre-extraction) or chromatin-bound proteins only (pre-extraction) (Figures 4.1B and C). In cells transfected with siPC4b and siPC4c, a very faint signal for PC4 was observed when compared with cells transfected with siCt, both with and without pre-extraction. These results indicated that the chosen antibody specifically recognizes PC4 without major cross-reactions with other proteins.

It was possible to observe that PC4 was evenly distributed throughout the nucleus in cells not subjected to pre-extraction (Figure 4.2A). A much weaker and punctate signal for PC4 was detected when pre-extraction was performed. In fact, to be able to clearly visualize the distribution of insoluble PC4, intensity settings had to be increased (Figure 4.2B). This indicates that only a small fraction of PC4 is chromatin bound (Figure 4.2A).

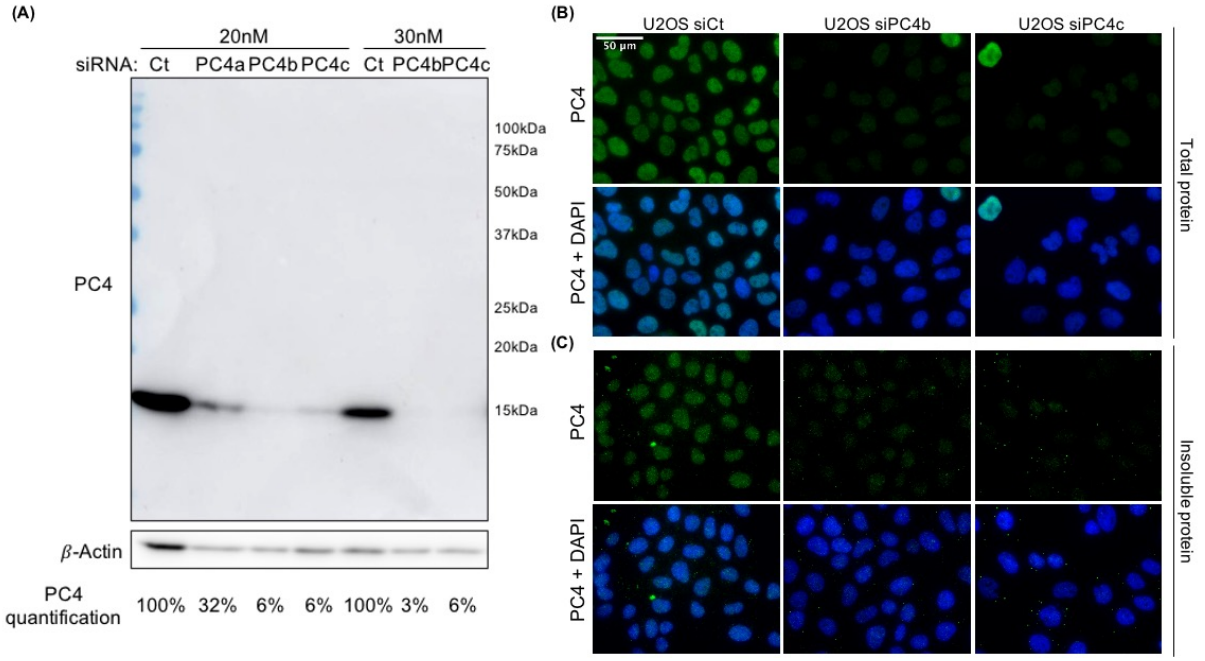

Figure 4.1 PC4 antibody validation. (A) Western blotting analysis of U2OS cells 72 h after transfection with 20 nM of siCt siPC4a, siPC4b and siPC4c and 30nM of siCt, siPC4b and siPC4c; (B) and (C) U2OS cells transfected with siRNAs (30nM) subjected to indirect immunofluorescence using antibodies against PC4 (green) for detection of (B) total proteins (without pre-extraction) and (C) insoluble proteins (with pre-extraction). DNA was counterstained with DAPI (blue).

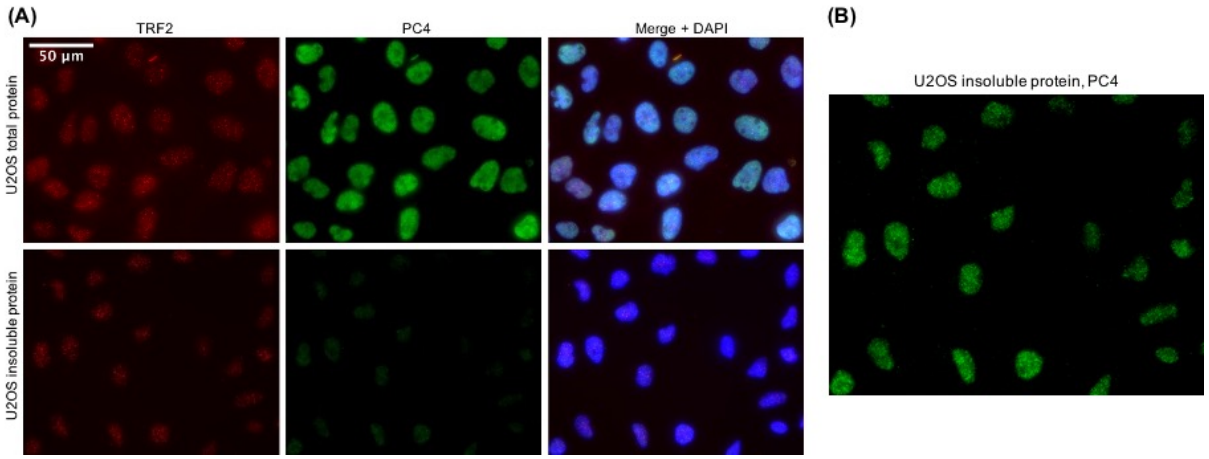

Figure 4.2 A fraction of PC4 is chromatin bound. U2OS cells subjected to indirect immunofluorescence using antibodies against TRF2 (to visualize telomeres; red) and PC4 (green). DNA was counterstained with DAPI (blue). (A) Comparison between total and insoluble protein, images for both conditions acquired with the same settings; (B) Image with adjusted intensity for insoluble PC4.

Knowing that a fraction of PC4 is bound to chromatin allowed me to further investigate if PC4 was present at telomeres using double IF for PC4 and the telomeric marker TRF2. Analysis of pre-extracted U2OS cells showed that PC4 localizes to the telomeres, as seen by the co-localization of PC4 foci with TRF2 foci (Figure 4.3A). Colocalization events were observed in the majority of cells analyzed. In fact, the number of colocalizations per cell ranged from 0 to 7, with only 13% of cells showing no co-localization of PC4 with TRF2, and a median of 2 colocalizations per cell (Figure 4.3B).

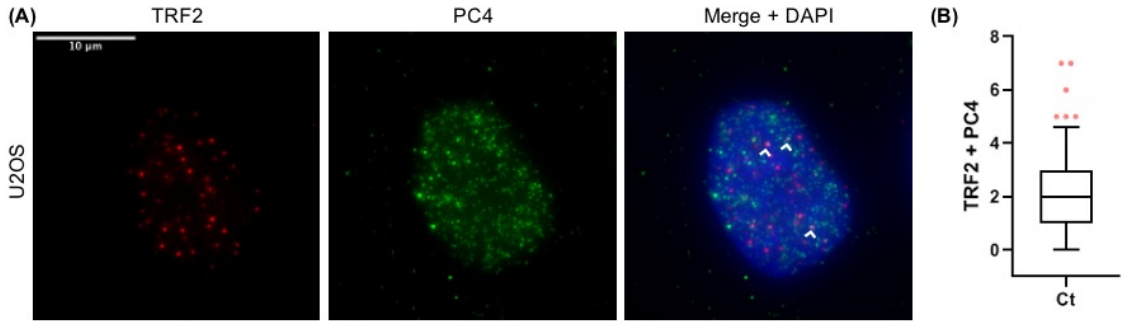

Figure 4.3 PC4 localizes to telomeres. (A) Representative image of U2OS cells subjected to indirect immunofluorescence using antibodies against TRF2 (to visualize telomeres; red) and PC4 (green). DNA was counterstained with DAPI (blue). Arrows indicate co-localizations between PC4 and TRF2; (B) Quantifications of numbers of co-localizations of PC4 with TRF2 per nucleus. A boxplot of the 10-90 percentile of values is shown. A total of 103 nuclei from one independent experiment were analyzed.

4.2 PC4 is recruited to the telomeres in response to replication stress

The conclusion that PC4 localizes to telomeres, together with studies that revealed increased recruitment of PC4 to DNA damage sites (97,101), led me to question if PC4 recruitment to telomeres could be stimulated/mediated by replication stress.

I first set up to reproduce the previous findings that PC4 recruitment to chromatin is increased by global replication stress induced by hydroxyurea (HU). In order to assess the localization of PC4 at telomeres, IF staining for PC4 and TRF2 was performed as above. An overall increase in PC4 association with chromatin was observed in HU treated cells (Figure 4.4A), most likely due to the induction of replication stress. HU treatment also increased recruitment of PC4 to telomeres (Figure 4.4A and B). A two-fold median increase in PC4 foci colocalizing with TRF2 per nucleus was observed, with very few nuclei without colocalizations and nuclei having as many as 17 colocalization events. These results allowed me to conclude that in response to generalized replication stress, PC4 is also recruited to telomeres.

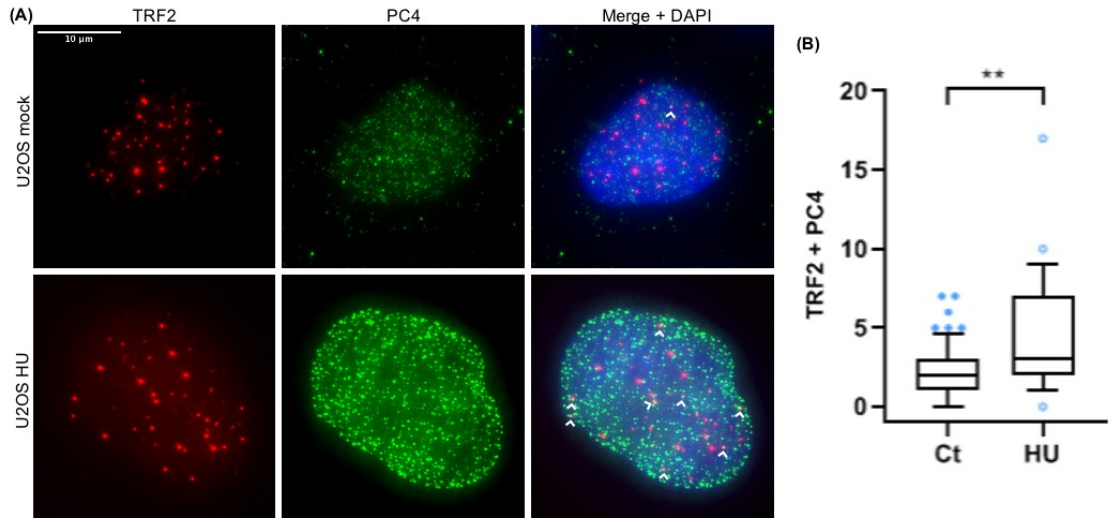

Figure 4.4 Replication stress induces recruitment of PC4 to both non-telomeric and telomeric chromatin. U2OS cells treated with 2 mM of HU for 24 h. (A) Examples of PC4 immunostaining (green) combined with TRF2 immunostaining (red) in U2OS cells for detection of insoluble protein. In the merge panel, DAPI-stained DNA is also shown (blue). Arrows indicate co-localizations between PC4 and TRF2; (B) Quantifications of numbers of co-localizations of PC4 with TRF2 per

nucleus. A total of at least 10 nuclei were analyzed from one independent experiment for each condition. A boxplot of the 10-90 percentile of values is shown. *P<0,05; **P<0,005; ***P<0,001; ****P<0,0001.

While HU treatment induces a generalized replication stress, the question that arises from these results is whether the induction of replication stress specifically at telomeres leads to the recruitment of PC4 to these structures. TRF1 averts replication defects at telomeres thus maintaining telomere stability (17,112). Four cell lines were chosen for this experiment, two ALT, U2OS and Saos-2, and two telomerase-positive, HOS and HeLa. TRF1 was depleted using a previously validated siRNA (112) and WB of total protein extracts was performed to confirm TRF1 knockdown (Figure 4.5A). While in U2OS, HOS and HeLa it was possible to clearly observe depletion of TRF1, in Saos-2 lower basal levels of TRF1 confounded the interpretation of the results. Hence, TRF1 depletion in this cell line was confirmed by RT-qPCR (Figure 4.5B).

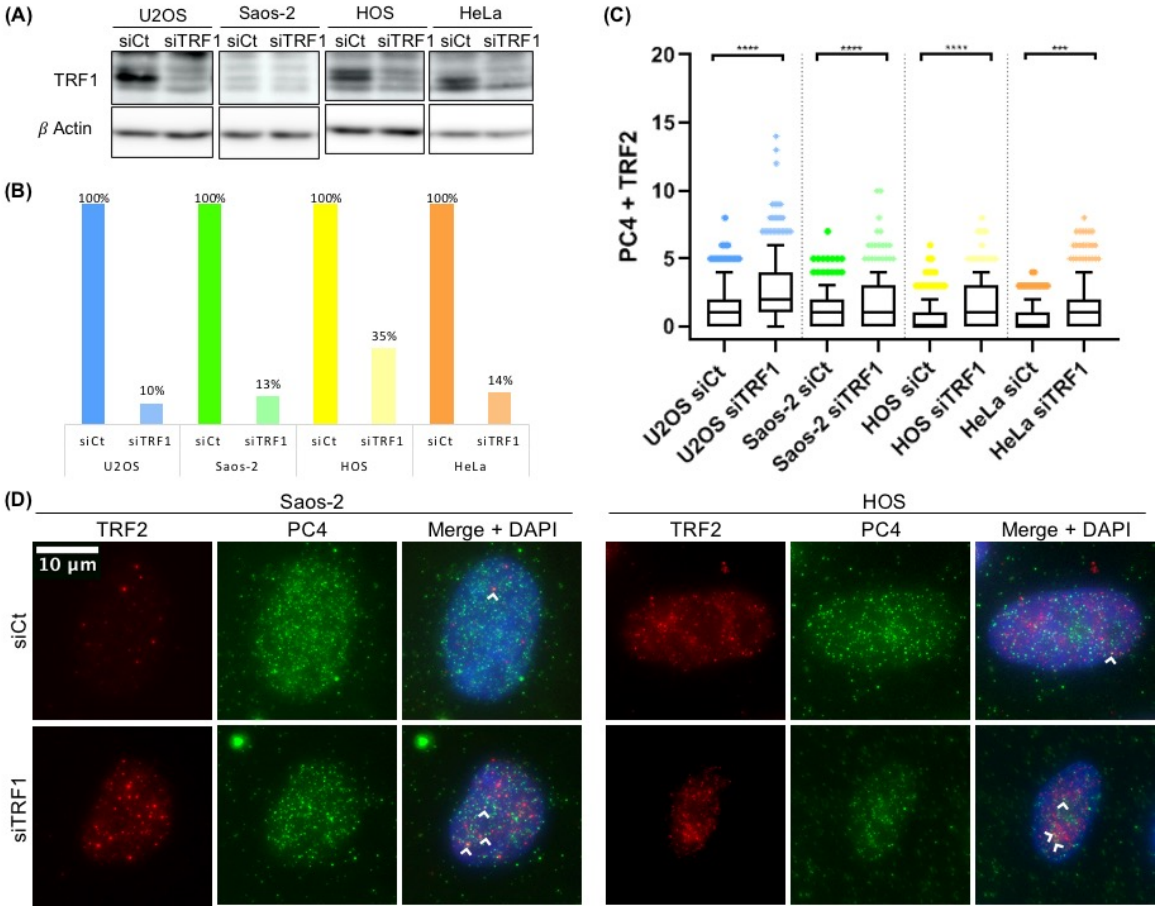

Figure 4.5 PC4 recruitment to telomeres upon telomeric replicative stress induction. (A) Western blotting analysis of U2OS, Saos-2, HOS and HeLa after 48 h of transfection with 20 nM of siCt or siTRF1; (B) RT-qPCR analysis of TRF1 mRNA in U2OS, Saos-2, HOS and HeLa after 48 h treatment with 20 nM of siTRF1; (C) Quantifications of numbers of co-localizations of PC4 with TRF2 per nucleus in U2OS, Saos-2, HOS and HeLa cells transfected with siTRF1 and harvested 48 h after transfection. Each dot represents an individual nucleus. A total of at least 100 nuclei from 3 independent experiments were analyzed for each sample. A boxplot of the 10-90 percentile of values is shown. *P<0,05; **P<0,005; ***P<0,001; ****P<0,0001; (D) Examples of PC4 immunostaining (green) combined with TRF2 immunostaining (red) in Saos-2 and HOS. In the merge panel, DAPI-stained DNA is also shown (blue). Arrows indicate co-localizations between PC4 and TRF2 (example of images for U2OS and HeLa cells in annex Figure 7.1B).

While the increase in telomere instability, due to depletion of TRF1, did not lead to a generalized increase in PC4 signal intensity, it led to a specific increase of PC4 at telomeres, as shown by an increase of PC4 colocalizing with TRF2 in all 4 cell lines (Figure 4.5D and annex Figure 7.1B).

Because ALT cells have increased ATRS, I questioned if PC4 is involved in the response to replication stress at ALT telomeres. As previously mentioned, FANCM and RNaseH1 are alleviators of ATRS and their depletion leads to exacerbated telomeric replication stress (50,51). RPA depletion in ALT cells also leads to accumulation of telomeric ssDNA, a signature of replication stress, while this does not occur in telomerase positive cells (113). Thus, the depletion of FANCM, RPA or RNaseH1 are good tools to study PC4 behavior in response to replication stress specifically occurring at ALT telomeres. I depleted those factors in the same 4 cell lines described above and confirmed protein depletion by WB; in the same cells, I performed a double-IF for PC4 and TRF2 (Figure 4.6 and annex Figure 7.1).

As previously reported (51,69), FANCM depletion led to formation of large telomeric clusters, as shown by large TRF2 foci, only in ALT cells (Figure 4.6C and annex Figure 7.1B). Also, ALT cells were characterized by large PC4 clusters co-localizing with TRF2 foci. The distribution of PC4 outside of telomeres did not seem to be affected by FANCM depletion (Figure 4.6C and annex Figure 7.1B).

Depletion of RPA70, one of the subunits of the RPA complex, had a milder effect on telomere clustering when compared to depletion of FANCM. While large TRF2 foci were still observed in ALT cells, and not in telomerase-positive cells, they were not as frequent as in ALT cells depleted for FANCM. Saos-2 also seemed to be more sensitive to RPA70 depletion than U2OS, as seen by a higher frequency of large TRF2 foci. Presence of PC4 clusters in these foci was also observed, both in U2OS and Saos-2. However, in contrast to FANCM depletion, RPA70 depletion in ALT cells increased not only the recruitment of PC4 to telomeres but also to non-telomeric chromatin, as showed by an increased intensity of pan-nuclear PC4 signal (Figure 4.6C and annex Figure 7.1B).

As previously reported, RNaseH1 depletion led to replication stress at telomeres (50), as shown by the accumulation of larger telomeric foci when compared with cells transfected with siCt. Similar to what was observed upon FANCM and RPA70 depletion, RNaseH1 depletion led to an increased co-localization of PC4 with telomeres in ALT cells but not in telomerase-positive cells. PC4 distribution outside telomeres did not seem to be affected by RNaseH1 depletion (Figure 4.6C and annex Figure 7.1).

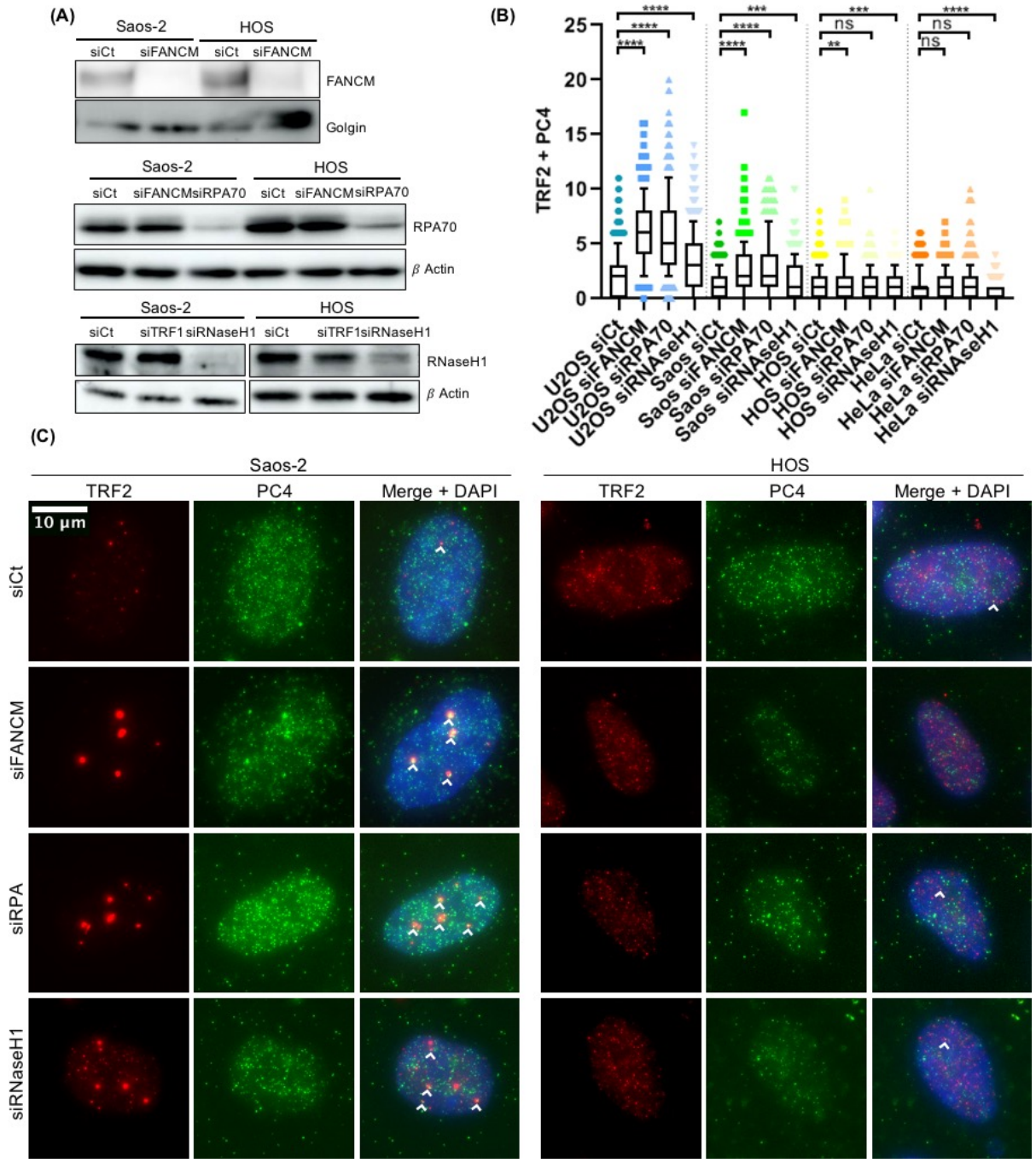

Figure 4.6 PC4 recruitment to ALT telomeres in response to replicative stress. (A) Western blotting analysis of Saos-2 and HOS after 48 h transfection with 20 nM of siCt, siFANCM, siRPA70 or siRNaseH1 (analysis of U2OS and HeLa in annex Figure 7.1A); (B) Quantifications of numbers of co-localizations of PC4 with TRF2 per nucleus in U2OS, Saos-2, HOS and HeLa. Each dot represents an individual nucleus. A total of at least 100 nuclei from 3 independent experiments were analyzed for each sample. A boxplot of the 10-90 percentile of values is shown. *P<0,05; **P<0,005; ***P<0,001; ****P<0,0001; (C) Examples of PC4 immunostaining (green) combined with TRF2 immunostaining (red) in Saos-2 and HOS. In the merge panel, DAPI-stained DNA is also shown (blue). Arrows indicate co-localizations between PC4 and TRF2 (example of images for U2OS and HeLa cells in annex Figure 7.1B).

4.3 PC4 localization at telomeres is partly dependent on RNA

The previous results show that PC4 is recruited to telomeres upon induction of replication stress. This advocates for the presence of PC4 interactors at telomeres. PC4 could bind to ssDNA, abundantly present at ALT telomeres due to telR-loop formation, through its ssDBD. PC4 has also been proposed to be a RNA binding protein (RBP) (84,109) and indeed one study has shown, through quantitative

interaction proteomics, that PC4 interacts with TERRA (110). This rises the hypothesis that PC4 could be recruited to telomeres in a TERRA-mediated manner.

First, I tested the possibility that PC4 binds to telomeric ssDNA in ALT cells. As previously mentioned, PC4 W89A is a mutant lacking the capability of binding to ssDNA due to the substitution of Trp89 in the β-ridge with Ala (80). I decided to induce replication stress at telomeres in ALT cells through FANCM depletion and test by IF if ectopically expressed PC4 W89A was recruited to telomeres. U2OS cells were infected with retroviruses expressing an siRNA-resistant Flag-tagged PC4 WT or PC4 W89A transgene. The PC4 cDNA was under the control of a CMV promoter. This system also allowed using an antibody against Flag, instead of the antibody against PC4, and thus validate the results previously obtained.

The expression of ectopic PC4 WT and W89A, as well as FANCM and endogenous PC4 depletion were confirmed by WB (Figure 4.7A). The quantification of protein band intensity showed that PC4 WT was expressed at around 30% and PC4 W89A at around 20% of the levels of endogenous PC4 in siCt transfected cells.

IF for TRF2 and Flag showed that depletion of FANCM led to the formation of large TRF2 foci in all three cell lines and that PC4 WT Flag was recruited to these big TRF2 foci (Figure 4.7B and C); as expected, no Flag signal was detected at telomeres in control U2OS EV cells transfected with siFANCM (Figure 4.7C). This result validates the observations made by IF using the PC4 antibody (Figure 4.6B). In PC4 W89A depleted for FANCM I also observed localization of Flag to the telomeric clusters, indicating that PC4 W89A still maintains the ability to be recruited to telomeres; this could be due the fact that recruitment does not requires ssDNA binding or to dimerization of PC4 W89A with endogenous PC4.

Depletion of endogenous PC4 in U2OS WT also led to some recruitment of Flag to telomeres (Figure 4.7B), which was expected since it was previously shown that PC4 localizes to the telomeres (Figure 4.3). The levels of recruitment of ectopic PC4 did not reach the ones observed with endogenous PC4, probably because of the lower expression of ectopic PC4 when compared with the endogenous. Depletion of endogenous PC4 in U2OS PC4 W89A also led to a minor recruitment of Flag to telomeres as in PC4 WT. Results obtained with depletion of endogenous PC4, in U2OS PC4 W89A, led me to discard the previous hypothesis of dimerization of PC4 W89A with endogenous PC4. In this experiment, endogenous PC4 was depleted from the cell, however the recruitment of PC4 W89A was still observed, suggesting that the ability of PC4 to bind to ssDNA might not be required for it to be recruited to the telomeres.

In order to test the hypothesis that PC4 association with telomeres is mediated by RNA, U2OS and Saos-2 cells depleted for FANCM were permeabilized and treated or not with RNaseA prior to cell fixation and IF. FANCM depletion was confirmed by WB (Figure 4.8A). As previously observed, depletion of FANCM led to the formation of large TRF2 foci containing PC4 (Figure 4.8B and annex Figure 7.2). When RNaseA treatment was performed, the large TRF2 foci were still visible, however

there was a significant decrease in PC4 localization within these foci (Figure 4.8B and C and annex Figure 7.2). These results suggest that PC4 recruitment to or maintenance at telomeres is at least in part mediated by RNA.

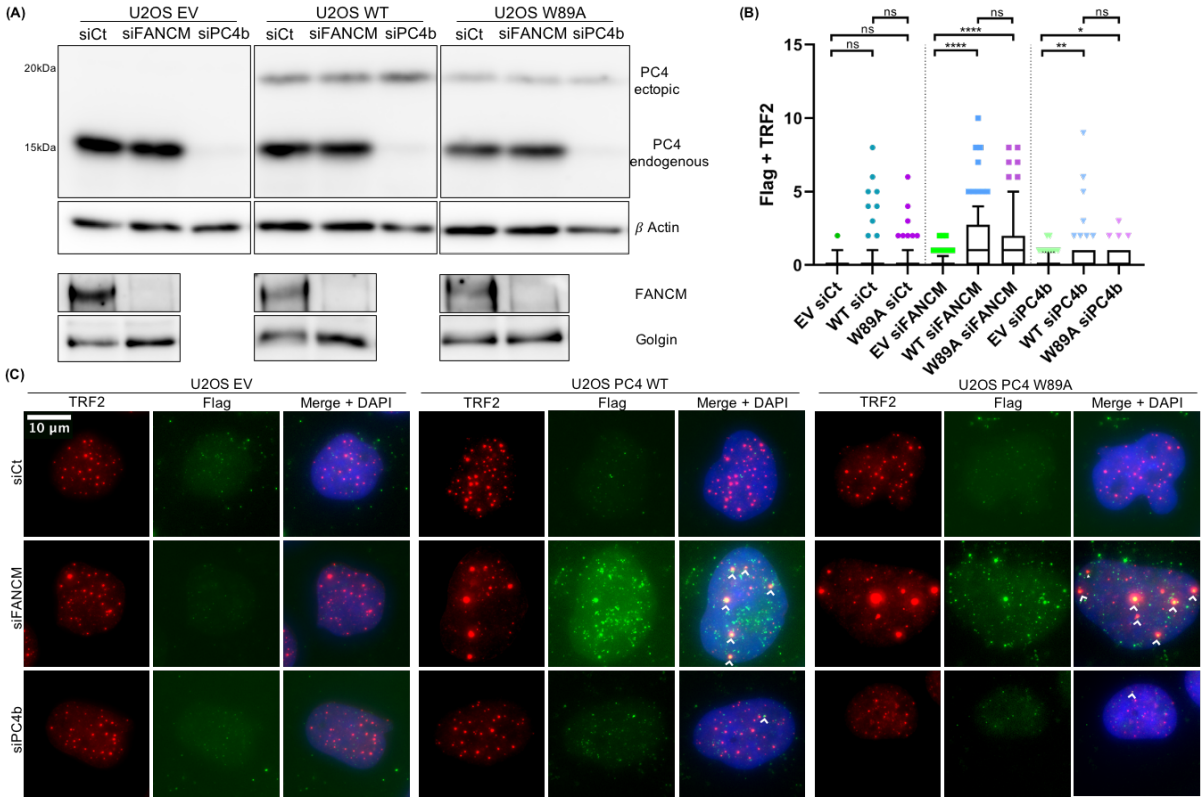

Figure 4.7 PC4 W89A mutant retains the ability to be recruited to the telomeres. (A) Western blotting analysis of U2OS EV, U2OS PC4 WT and U2OS PC4 W89A after 48 h transfection with 20 nM of siCt or siFANCM or 30 nM of siPC4b; (B) Quantifications of numbers of co-localizations of Flag with TRF2 per nucleus in U2OS EV, U2OS PC4 WT and U2OS PC4 W89A. Each dot represents an individual nucleus. A total of at least 100 nuclei from 1 experiment were analyzed for each sample. A boxplot of the 10-90 percentile of values is shown. *P<0,05; **P<0,005; ***P<0,001; ****P<0,0001; (C) Examples of Flag immunostaining (green) combined with TRF2 immunostaining (red) in U2OS EV, U2OS PC4 WT and U2OS PC4 W89A. In the merge panel, DAPI-stained DNA is also shown (blue). Arrows indicate co-localizations between Flag and TRF2.

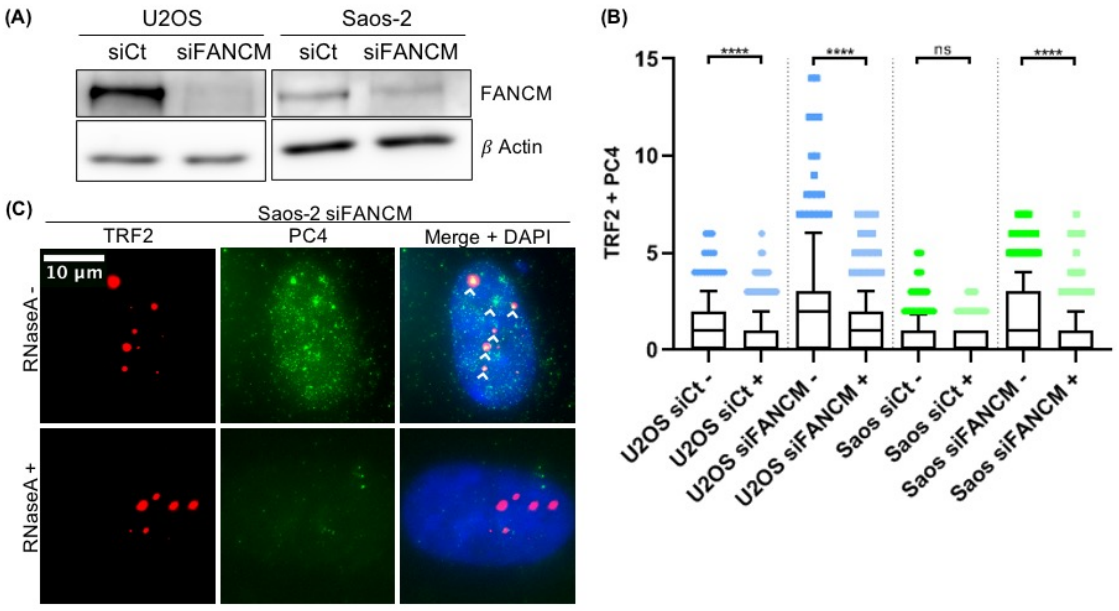

Figure 4.8 PC4 localization at telomeres is dependent on RNA. (A) Western blotting analysis of U2OS and Saos-2 after 48 h transfection with 20 nM of siCt or siFANCM; (B) Quantification of numbers of co-localizations of PC4 with TRF2 per nucleus in U2OS and Saos-2, without treatment (-) and with treatment (+) with RNaseA before fixation. Each dot represents an individual nucleus, a total of at least 100 nuclei from 3 independent experiments were analyzed for each sample (U2OS siFANCM results report to 2 independent experiments instead of 3). A boxplot of the 10-90 percentile of values is shown. *P<0,05; **P<0,005; ***P<0,001; ****P<0,0001; (C) Examples of PC4 immunostaining (green) combined with TRF2 immunostaining (red) in Saos-2 siFANCM (example of images for U2OS siFANCM in annex Figure 7.2). In the merge panel, DAPI-stained DNA is also shown (blue). Arrows indicate co-localizations between PC4 and TRF2.

4.4 PC4 depletion affects telomere integrity in ALT cells

Because PC4 associates with ALT telomeres, I set up to test whether it supports telomere integrity by performing IF for TRF2 combined with markers of DNA damage, RPA32 phosphorylated at serine 33 (pSer33) and histone H2AX phosphorylated at serine 139 (γH2AX). Replication fork stalling, during S phase, leads to phosphorylation of RPA32 by ATR while DSBs lead to phosphorylation of H2AX by ATM (114,115).

Depletion of PC4 was performed using both siPC4b and siPC4c, in order to confirm that any telomeric changes were specifically due to PC4 depletion. Depletion of PC4, with both siRNAs, led to accumulation of pSer33 at telomeres in U2OS and Saos-2 cells (Figure 4.9). Accumulation of pSer33 at telomeres in depleted HOS cells was not observed. These results suggest a buildup of replication stress at telomeres in ALT cells due to PC4 depletion. Depletion of PC4 also led to an even more remarkable increase of γH2AX at telomeres in ALT cells (Figure 4.10). In HOS no rise in γH2AX accumulation at telomeres was observed upon PC4 depletion.

The accumulation of pSer33 and γH2AX at telomeres in PC4 depleted cells strongly suggests that PC4 averts replication stress and DNA damage at ALT telomeres.

Because PC4 is a transcriptional factor, its depletion could affect the transcription of mRNAs coding for shelterin proteins, and changes in shelterin protein levels could be the cause of the telomere instability observed upon depletion of PC4. To test this hypothesis, U2OS, Saos-2, HOS and HeLa were transfected with siPC4b and shelterin protein levels were assessed by WB using protein extracts collected 72 h after transfection (Figure 4.11). No major change in POT1, TRF2, TPP1, Rap1, TRF1 and TIN2 levels were observed in ALT and telomerase positive cells depleted for PC4. Thus, I concluded that the telomere instability observed in ALT cells depleted of PC4 must have a cause other than altered shelterin levels.

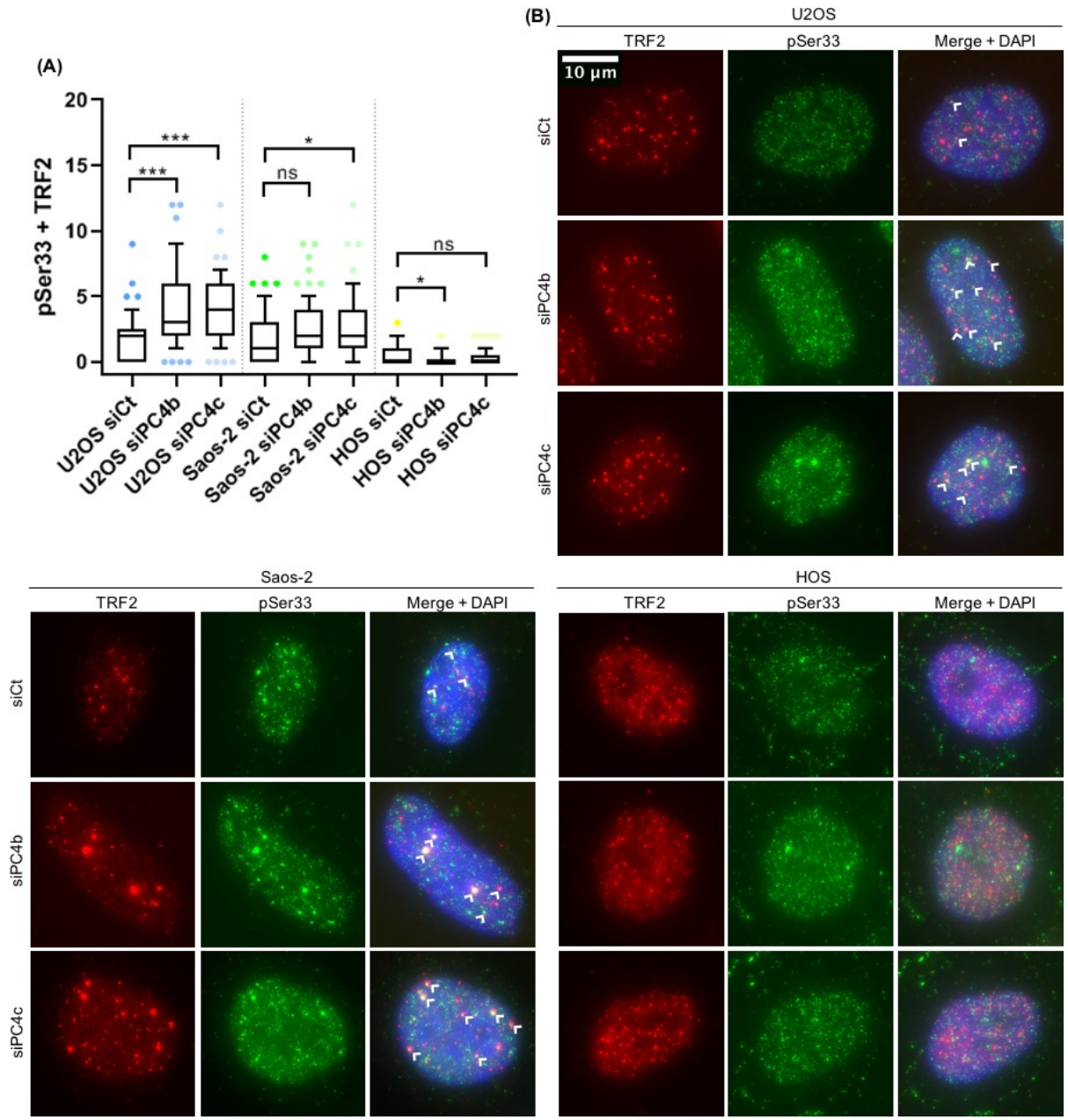

Figure 4.9 pSer33 at telomeres in PC4-depleted cells. (A) Quantification of numbers of co-localizations of pSer33 with TRF2 per nucleus in U2OS, Saos-2 and HOS cells transfected with 30 nM of siCt, siPC4b and siPC4c for 72 h. Each dot represents an individual nucleus, a total of at least 100 nuclei from 1 experiment were analyzed for each sample. A boxplot of the 10-90 percentile of values is shown. *P<0,05; **P<0,005; ***P<0,001; ****P<0,0001; (B) Examples of pSer33 immunostaining (green) combined with TRF2 immunostaining (red) in U2OS, Saos-2 and HOS. In the merge panel, DAPI-stained DNA is also shown (blue). Arrows indicate co-localizations between pSer33 and TRF2.

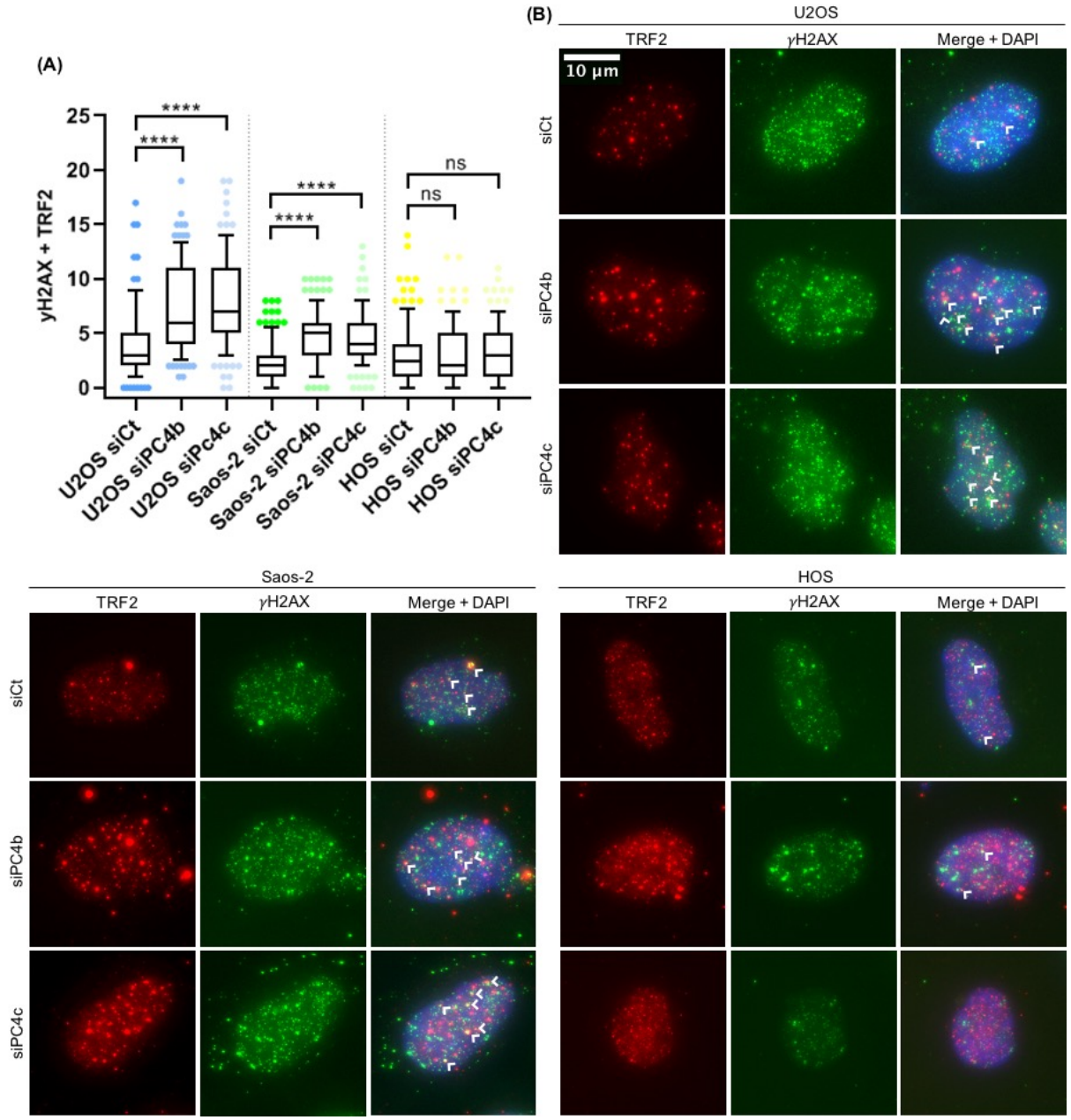

Figure 4.10 γH2AX at telomeres in PC4-depleted cells. (A) Quantification of numbers of co-localizations of γH2AX with TRF2 per nucleus in U2OS, Saos-2 and HOS cells transfected with 30 nM of siCt, siPC4b and siPC4c for 72 h. Each dot represents an individual nucleus, a total of at least 100 nuclei from 1 experiment were analyzed for each sample. A boxplot of the 10-90 percentile of values is shown. *P<0,05; **P<0,005; ***P<0,001; ****P<0,0001; (B) Examples of γH2AX immunostaining (green) combined with TRF2 immunostaining (red) in U2OS, Saos-2 and HOS. In the merge panel, DAPI-stained DNA is also shown (blue). Arrows indicate co-localizations between γH2AX and TRF2.

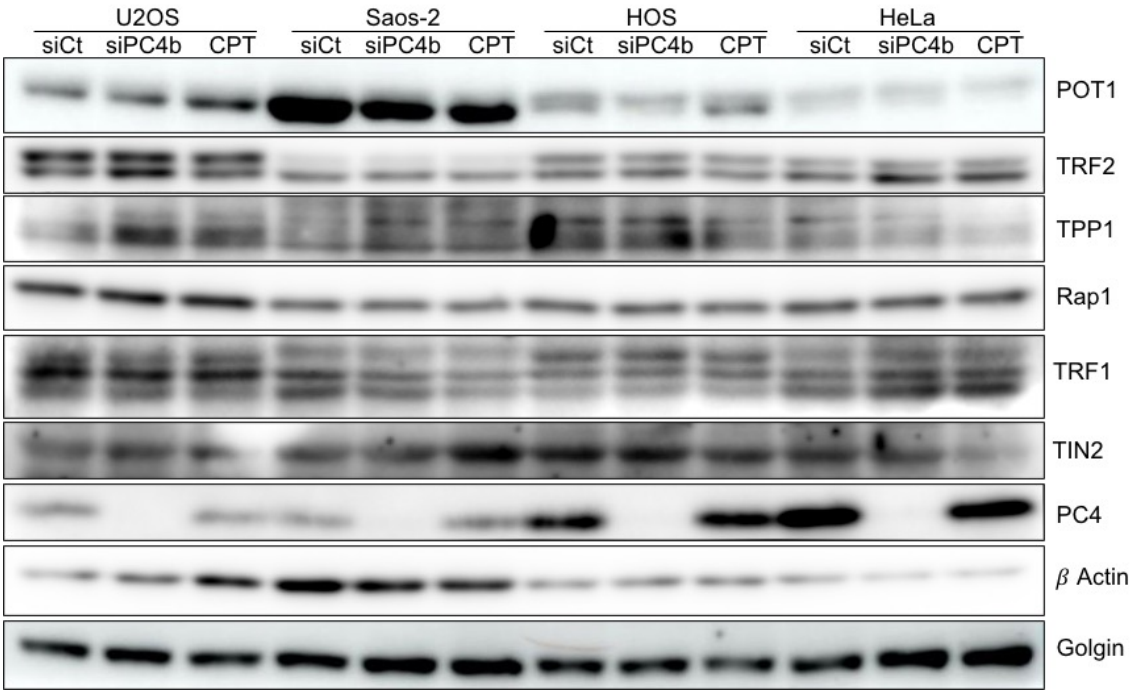

Figure 4.11 Shelterin protein levels in PC4-depleted cells. Western blotting analysis of U2OS, Saos-2, HOS and HeLa 72 h after transfection with siCt or siPC4b. Untransfected cells treated with camptothecin (CPT) were included to control for antibody specificity.

4.5 PC4 supports ALT cells viability

Telomere instability in ALT cells depleted for PC4 could have consequences on cell fitness. To test whether PC4 is involved in supporting ALT cell viability, I followed cell proliferation in PC4 depleted cells. PC4 was continuously depleted with siPC4b and siPC4c in U2OS, Saos-2, HOS and HeLa cells and cell numbers were counted every 3 days for 2 weeks.

ALT cell lines lost their ability to proliferate and started dying after depletion of PC4 (Figure 4.12 and annex Figure 7.3). The proliferation of telomerase positive cells was not majorly affected during the tested time course (Figure 4.12 and annex Figure 7.3). This suggests that telomere instability observed in ALT cells, upon depletion of PC4, might lead to cell death.

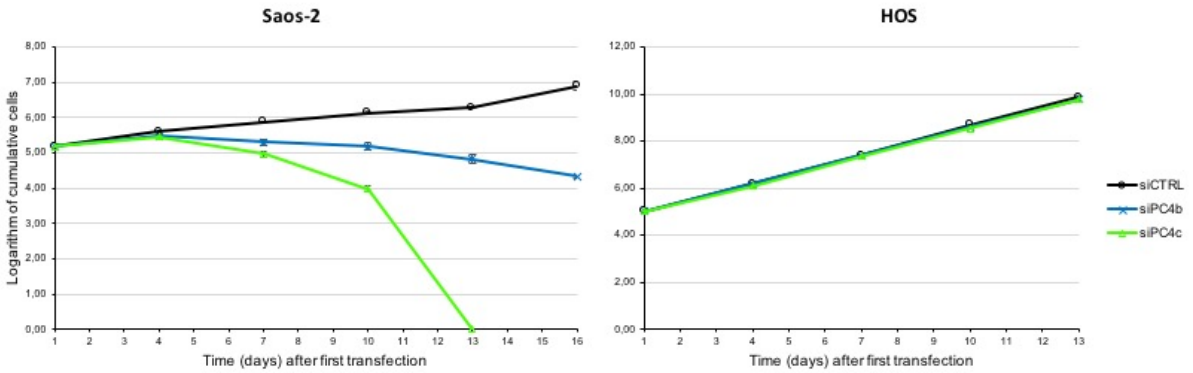

Figure 4.12 Growth Curves of PC4-depleted cells. Cellular proliferation of Saos-2 and HOS after transfection with 30 nM of siCt, siPC4b and siPC4c (graphics for U2OS and HeLa in annex Figure 7.3) every 3 days. Cumulative cell numbers are expressed in a logarithmic transformation of base 10. Data points and error bars are means and SDs from 3 independent experiments.

The proliferation of ALT cells was slightly different when using siPC4b or siPC4c. Depletion using siPC4c led to an earlier loss of cells and death of the entire cell population in both Saos-2, 13 days after first transfection, as in U2OS, 7 days after transfection (Figure 4.12 and annex Figure 7.3). Depletion with siPC4b in Saos-2 was not performed long enough to reach cell death of the entire cell population (Figure 4.12), while in U2OS full cell death was reached 6 days later than with siPC4c, 13 days after first transfection (annex Figure 7.3). Considering that depletion of PC4 with siPC4b is more efficient than siPC4c (Figure 4.3A) this might mean that siPC4c has some off-targets anticipating cell death.

To address the possibility of off-target effects associated with siPC4c, I decided to complement Saos-2 cells with siRNA-resistant PC4 WT. A rescue in cell death would confirm specificity of the siRNAs and eliminate the possibility of off-target effects. Saos-2 cells over-expressing an siRNA-resistant PC4 WT were generated by infection with retroviruses expressing a Flag-PC4 WT transgene from a LTR promoter. Ectopic PC4 expression was very low when compared with endogenous PC4, around 5% (Figure 4.13A); nevertheless, I decided to perform growth curves with these cells since even low expression of ectopic PC4 could be enough to avert cell proliferation defects.

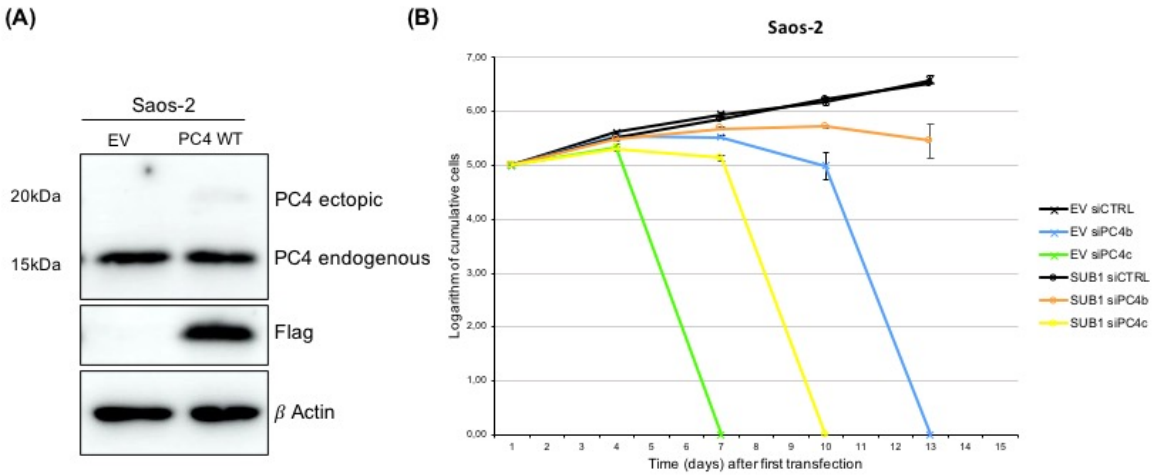

Figure 4.13 Growth curves of PC4-depleted cells with PC4 complementation. (A) Western blotting analysis of U2OS and Saos-2 six days after first infection; (B) Cellular proliferation of Saos-2 EV and Saos-2 WT PC4 after transfection with 30 nM of siCt, siPC4b or siPC4c. Cumulative cell numbers are expressed in a logarithmic transformation of base 10. Data points and error bars are means and SDs from 3 independent experiments.

Saos-2 PC4 WT showed a better fitness, being the decrease in proliferation slower than in Saos-2 EV, when depletion was performed with siPC4b (Figure 4.13B). Since Saos-2 PC4 WT had only 5% expression of ectopic PC4, this could mean that the ectopic PC4 was not enough to fully compensate for depletion of endogenous PC4. When PC4 was depleted with siPC4c, a similar growth decrease was observed in Saos-2 EV and Saos-2 PC4 WT, total population death was reached with a delay of 3 days. This similar growth after treatment with siPC4c, associated with a lower efficiency of siPC4c when compared to siPC4b, does suggest the existence of off-target effects. However, it will be important to repeat this experiment using cell lines with higher expression of ectopic PC4.

My results indicate that ALT cells lose their proliferative potential and start dying after PC4 depletion. Since in this work I had used a limited panel of ALT cells, I took advantage of an open source tool, the Achilles Project Database, to corroborate these results. The Achilles Project is an online platform which collects information of gene dependency in a vast panel of human cancer cells. This dependency is determined after knockout or knockdown of genes in different cell lines, using Crispr-Cas9, siRNAs or shRNAs. I used this platform to do a search for PC4 dependency in a list of 6 known ALT cell lines (U2OS, Saos-2, CAL72, CAL78, G292 and SKLU1). It is important to note that other cell lines in the database could also be ALT, however they might have not been characterized as such yet. First, a general analysis of PC4 dependency was performed through Gene Effect (CERES) (Figure 4.14A). CERES dependency score is based on assays from CRISPR (Avana) Public 20Q3 dataset. A low CERES score indicates a higher likelihood that the gene of interest is essential in a given cell line (e.g. a score of 0 indicates the gene is not essential, a score of -1 is comparable to the median of all pan-essential genes). All known ALT cell lines have a PC4 CERES dependency score below -0,5, suggesting a dependency of these ALT cell lines on PC4 (Figure 4.14A). On the other hand, two known telomerase positive cell lines, HT1080 (116) and A549 (117), have a score close to 0, further hinting to a dependency of PC4 specific to ALT cells. In the 777 cell lines present in the dataset, only 29 have a PC4 CERES score below -0,5, and five of these have origin in bone (Figure 4.14B). ALT is more frequently found in bone tumors, and indeed the ALT cell lines used in this study, U2OS and Saos-2, originated from osteosarcoma. These results support the notion that PC4 is important for ALT cell survival.

These results raise then the question of what mechanism is responsible for the death of ALT cells in the absence of PC4. Two major pathways for cell death are apoptosis and autophagy. Apoptosis, or programmed cell death, can occur normally during development and aging or can be triggered by cellular damage (118,119). Autophagy is a self-degradation process, that possesses a role in prevention of diseases like cancer (120). Poly(ADP-ribose) polymerase (PARP) is a 113 kDa nuclear enzyme that is cleaved by caspases 3 and 7 in fragments of 89 and 24 kDa during apoptosis (121) and can be used as an apoptosis marker. On the other side, microtubule-associated protein 1 light chain 3 (LC3B) is a commonly used marker for autophagy. LC3B-I is converted into LC3B-II through conjugation of cytosolic LC3B-I to phosphatidylethanolamine (PE) on the surface of nascent autophagosomes (122).

I transfected U2OS, Saos-2, HeLa and HOS cells with siPC4b or siCt and performed immunodetection of PARP and LC3B by WB using total protein extracts prepared 72 h after transfection.

I observed that full-length PARP (FL-PARP) levels did not change after PC4 depletion, as well as the 89 kDa cleaved PARP (C-PARP) (Figure 4.15). This indicates that cells are not undergoing apoptosis upon PC4 depletion, at least at the tested timepoint.

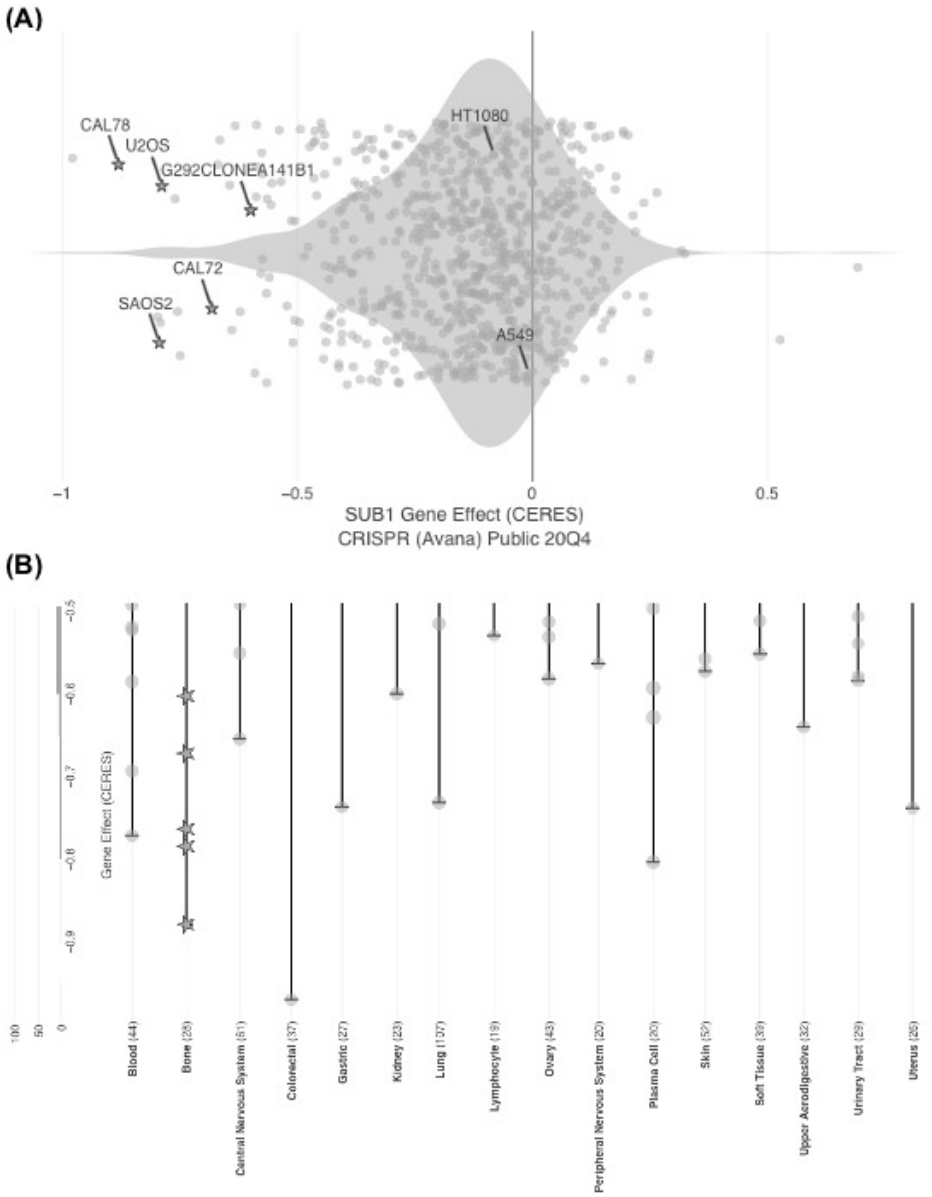

Figure 4.14 Achilles project. (A) CERES dependency score for PC4 (SUB1) in 777 cell lines, stars mark known ALT cell lines, HT1080 and A549 are telomerase-positive cell lines; (B) Distribution of PC4 CERES dependency score below -0,5 for 777 cell lines, stars represent known ALT cell lines.

In ALT cells I observed a decrease in LC3B-I, decrease of 17% in U2OS and 47% in Saos-2. A 38% increase in LC3B-II was observed in U2OS cells. Both telomerase-positive cells also had a decrease in LC3B-I, 32% in HOS and 11% in HeLa, but this was also accompanied by a decrease in LC3B-II, 20% in HOS and 15% in HeLa. These changes in LC3B-I and -II ratios may suggest that autophagy is triggered by PC4 depletion, likely only in ALT cells considering the growth curve results. However, further analyses need to be performed using longer times of PC4 depletion as the effects of PC4 depletion on cell proliferation only start to be clear by day 7 (Figure 4.12).

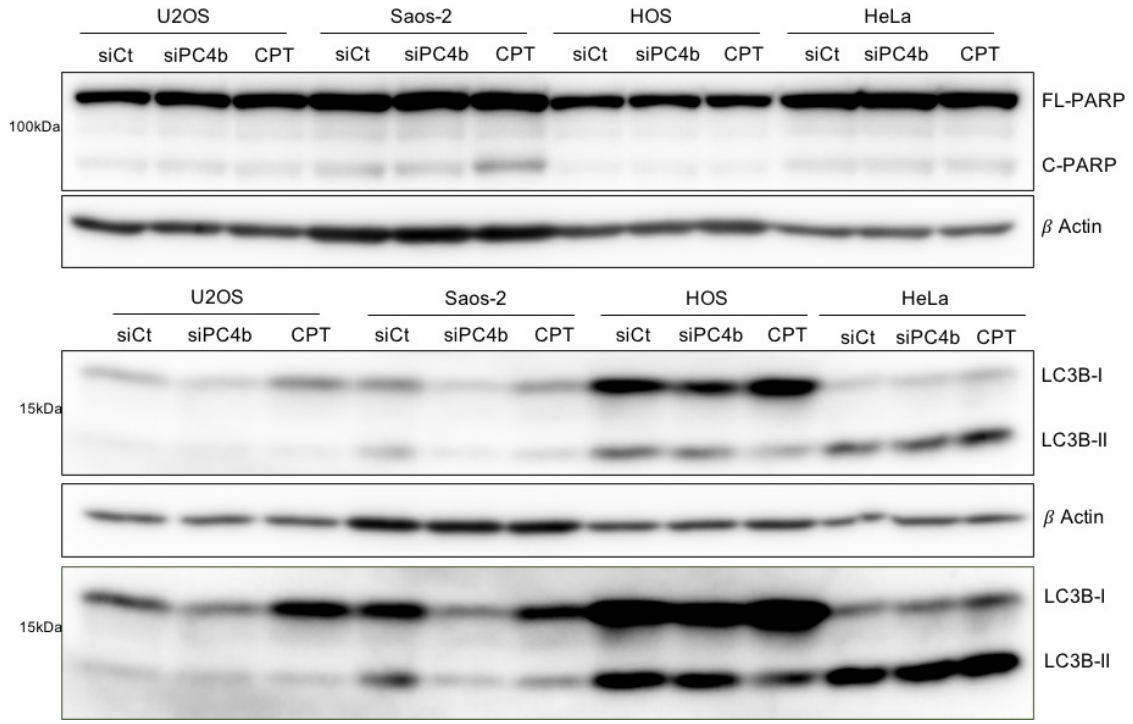

Figure 4.15 Assessment of autophagy and apoptosis in PC4-depleted cells. Western blotting analysis of U2OS, Saos-2, HOS and HeLa 72 h after treatment with siCt or siPC4b. Untransfected cells treated with camptothecin (CPT) were included to control for antibody specificity. Lower panel with higher contrast to allow better observation of ALT cell lines.

5. Conclusion

PC4 is a protein with diverse cellular functions ranging from transcription to replication, genome stability and chromatin organization. Here I demonstrate, by immunostaining, that PC4 is mainly soluble in the nucleoplasm, while only a small fraction of this protein is found bound to chromatin. A fraction of chromatin bound PC4 can be found at telomeres, as shown by colocalization of PC4 with the telomeric factor TRF2. This suggests a function for PC4 at telomeres.

Hydroxyurea is widely used to treat multiple diseases. Its action leads to inhibition of DNA synthesis and it can lead to DNA damage and cell cycle arrest in a concentration and time-dependent manner (123). Stimulation of replication stress in cells, through hydroxyurea, produced an overall increase of PC4 on chromatin. These results agree with previous findings that PC4 has a role in the stimulation of DSB repair through HR (102). PC4 increased accumulation upon hydroxyurea treatment was also observed at telomeres, further supporting a possible role for PC4 in alleviating telomeric replication stress.

Depletion of TRF1, a telomeric protein supporting telomeric DNA replication, was used as a model to introduce replication stress specifically at telomeres (112). I found that an increase in telomeric stress led to enhanced recruitment of PC4 to telomeres. This was showed in four different cell lines in three independent experiments. Future experiments could use different approaches to induce telomere instability, like depletion of TRF2. However, in this case it would not be possible to assess PC4 recruitment to telomeres through the same method used, IF for PC4 and TRF2. IF should be performed

for PC4 in conjunction with TRF1 or be replaced by IF combined with fluorescence *in situ* hybridization to detect telomeric DNA.

ALT cells, in order to elongate their telomeres through homology-direct repair, maintain their telomeres physiologically damaged. Knowing that PC4 association with telomeres increases when replication stress is induced, I thought that PC4 could have an important role in replication stress at ALT telomeres. I exploited known ATRS alleviators, FANCM, RNaseH1 and RPA (50,51) (113), to answer this question. Depletion of FANCM, RPA70 and RNaseH1 led to an increase of ATRS, as shown by more intense and larger TRF2 foci possibly originating from telomere clustering (51). Increased ATRS, in all three conditions, was accompanied by an increase in PC4 recruitment to telomeres. This could indicate that besides FANCM and RNaseH1, PC4 has a role as an ATRS alleviator, keeping stress at telomeres within controlled ranges, thereby averting too elevated levels of DNA damage that would lead to cell proliferation arrest and death.

To further characterize and understand PC4 roles at telomeres, it is important to understand how it is recruited. PC4 binds, in an unspecific manner, to dsDNA through its N-terminal domain. Binding to ssDNA and partly melted dsDNA is mediated by PC4 C-terminal domain (PC4 CTD). The ability to bind to pre-mRNA was also characterized through a universal protein array (84). Previous studies also showed that PC4 can interact with G4s structures, in a different manner from the one it interacts with ssDNA or partly melted DNA. G4s can occur in dsDNA, ssDNA or even in RNA. When G4s occurs in dsDNA, while one monomer of the PC4 dimer binds to the G4 strand, the other monomer is bound to the C-rich strand that is displaced (83). However, it is important to keep in mind that TERRA, being rich in guanines, also tends to form G4s.

Various PC4 mutant proteins have been used to understand how PC4 behaves and what domains are responsible for each of its functions. PC4 W89A cannot interact with ssDNA and heteroduplex structures partially melted (76). It is unknown if PC4 W89A is able to dimerize with PC4 WT, however it is likely since the ssDNA binding domain and dimerization domain are separate (87). Upon depletion of endogenous PC4, small amounts of ectopic PC4 W89A and PC4 WT co-localized with TRF2 foci, suggesting that both proteins retain the ability to be recruited to telomeres. Moreover, PC4 W89A was detected at ALT telomeres upon telomeric replication stress by depletion of FANCM. These results could argue for a PC4 ssDBD-independent recruitment to telomeres, however further experiments need to be performed. Only one experiment was executed, and the expression of ectopic protein was not ideal. Protein over-expression needs to be improved as ectopic expression of PC4 WT was less than 30% when compared with endogenous PC4. Additionally, expression of PC4 W89A was 10% lower than PC4 WT and this could further confound the interpretation of the results.

Other cell lines can also be developed to investigate the region of PC4 responsible for its recruitment. For example, complementation with PC4-N (C-terminal deletion) could establish if PC4 CTD is necessary for PC4 recruitment to telomeres, and complementation with PC4 CTD (N-terminal deletion) could indicate if CTD in sufficient for PC4 recruitment. Other truncated/mutated PC4 proteins

could also be tested, including substitutions of CkII sites (PC4-ΔS), since it was shown that P-PC4 had increased DNA-binding activity (84).

A previous study based on quantitative interaction proteomics suggested that PC4 is a TERRA interactor (110). Given that TERRA annealing with telomeric DNA is a trigger of ATRS, I questioned if PC4 could be recruited to telomeres through TERRA. Treatment with RNaseA, which degrades ssRNA, was performed before cell fixation. PC4 recruitment, in conditions of increased telomeric stress, strongly decreased upon RNaseA treatment without being completely abolished. This treatment did not affect the large TRF2 foci. These results, obtained in two different ALT cell lines, suggest that PC4 recruitment to telomeres is at least in part mediated by RNA.

An *in vitro* study, using recombinant human PC4 purified from bacteria, showed that non-phosphorylated PC4 is able to bind to RNA (84). However, none of the PC4 point mutants tested affected PC4 RNA binding ability, including mutants affecting ssDNA binding other than W89A. This supports our findings that PC4 recruitment to telomeres is at least in part mediated by RNA and PC4 W89A retains the capability to bind telomeric molecules. Further experiments should answer if PC4 can interact specifically with TERRA or if it binds to RNA in a non-specific manner. Electrophoretic mobility shift assay (EMSA) can be used to test PC4 binding to TERRA. It would also be interesting to bring truncated/mutated PC4 proteins into this context, like PC4 W89A and PC4-ΔS, since little is known about PC4 RNA binding activity.

Another approach that can be used to test TERRA-mediated recruitment of PC4 to telomeres is to exploit U2OS cell lines expressing Transcription Activator-Like Effectors (TALEs) previously engineered in the lab (unpublished data). These TALEs bind specifically to the 29bp CpG islands which contain TERRA promoters. TALEs were further fused to a transcription repressor domain or a transcription activator domain in order to modulate TERRA transcription in cells. Using these cells lines to perform IF for PC4 and TRF2 would permit testing if TERRA levels affect PC4 recruitment to telomeres.

I demonstrated that PC4 depletion affects telomere integrity in ALT cells. The DNA damage markers, pSer33 and γH2AX, accumulated at telomeres upon depletion of PC4. This was exclusive to ALT cells and not observed in telomerase-positive HOS cells. This preliminary data needs to be further confirmed, with a larger cell line panel and independent repetitions of the experiment.

PC4 depletion could lead to telomere instability by affecting shelterin protein levels. However, PC4 depletion did not affect the cellular levels of the six shelterin components, indicating that telomere instability must be caused by a different defect. If PC4 is an ATRS alleviator, its depletion would lead to accumulation of replication stress and telomere instability. This hypothesis could be tested by verifying if PC4 depletion leads to higher levels of ALT features, like APBs or C-circles. Another approach would be to over-express PC4 in ALT cells and determine if telomere shortening occurs, which is expected if ATRS and telomeric recombinogenic potential decline, similarly to what happens when

RNaseH1 is overexpressed in ALT cells (50). For these studies, an experimental setup allowing strong over-expression of PC4 would be necessary, pointing to the importance of developing of new and efficient over-expression systems.

The present study also shows that PC4 is important for ALT cell viability. Knockdown of PC4 in two different ALT cell lines led to loss of proliferation and cell death, while the two chosen telomerase-positive cell lines were not majorly affected. Future experiments, with cell lines expressing significant levels of ectopic PC4, would be important to demonstrate if PC4 WT expression is able to fully avert the phenotype. It would also be interesting, keeping in consideration the results obtained with PC4 W89A recruitment to telomeres, to understand if PC4 W89A is able to compensate for the proliferation loss upon PC4 depletion. Again, other mutated or truncated proteins could also be used to further detail which PC4 domains are important for ALT cell viability.

Finally, my results seem to point to autophagy activation upon depletion of PC4, possibly leading to ALT cell death. These are very preliminary results and need to be investigated in settings where longer PC4 depletion times are used. Cell proliferation loss is more evident at 7 days after the first transfection, both in U2OS and Saos-2, while my experiments to test autophagy activation were performed with extracts collected 3 days after transfection. Future experiments should also be performed in PC4 depleted ALT cells treated with agents blocking lysosome degradation; this will allow to study autophagy flux rather than steady state levels of autophagy markers.

In conclusion, this study provides a solid foundation for a novel role of PC4 in the ALT mechanism, potentially as an ATRS alleviator. Further studies in this direction will ascertain whether PC4 could represent a new target for future therapeutic approaches to cure ALT cancers. This can be approached in two different manners. PC4 activity can be enhanced leading to a decrease in telomere replication stress and loss of recombinogenic potential, resulting in replicative senescence, due to an inability to elongate telomeres. Conversely, PC4 activity can be abolished, possibly combined with other ATRS alleviators (such as FANCM), which will lead to increased telomere instability and hasty cell death.

6. Bibliography

1. McClintock B. The Stability of Broken Ends of Chromosomes in Zea Mays. Genetics [Internet]. 1941;26(2):234–82. Available from: http://www.ncbi.nlm.nih.gov/pubmed/17247004%0Ahttp://www.pubmedcentral.nih.gov/articlerender.fcgi?artid=PMC1209127
2. Blackburn EH, Greider CW, Szostak JW. Telomeres and telomerase: The path from maize, Tetrahymena and yeast to human cancer and aging. Nat Med. 2006;12(10):1133–8.
3. Blackburn EH, Gall JG. A tandemly repeated sequence at the termini of the extrachromosomal ribosomal RNA genes in Tetrahymena. J Mol Biol. 1978;120(1):33–53.
4. Szostak JW, Blackburn EH. Cloning yeast telomeres on linear plasmid vectors. Cell. 1982;29(1):245–55.
5. Moyzis RK, Buckingham JM, Cram LS, Dani M, Deaven LL, Jones MD, et al. A highly conserved

repetitive DNA sequence, (TTAGGG)(n), present at the telomeres of human chromosomes. Proc Natl Acad Sci U S A. 1988;85(18):6622–6.

6. Meyne J, Ratliff RL, Moyzis RK. Conservation of the human telomere sequence (TTAGGG)(n) among vertebrates. Proc Natl Acad Sci U S A. 1989;86(18):7049–53.
7. Hayflick L, Moorhead PS. The serial cultivation of human diploid cell strains. Exp Cell Res. 1961;(25):585–621.
8. Olovnikov AM. Principle of marginotomy in template synthesis of polynucleotides. Dokl Akad Nauk SSSR [Internet]. 1971;201(6):1496–9. Available from: http://www.ncbi.nlm.nih.gov/pubmed/5158754
9. Sandell LL, Zakian VA. Loss of a yeast telomere: Arrest, recovery, and chromosome loss. Cell. 1993;75(4):729–39.
10. Makarov VL, Hirose Y, Langmore JP. Long G tails at both ends of human chromosomes suggest a C strand degradation mechanism for telomere shortening. Cell. 1997;88(5):657–66.
11. Griffith JD, Comeau L, Rosenfield S, Stansel RM, Bianchi A, Moss H, et al. Mammalian telomeres end in a large duplex loop. Cell. 1999;97(4):503–14.
12. Hirashima K, Seimiya H. Telomeric repeat-containing RNA/G-quadruplex-forming sequences cause genome-wide alteration of gene expression in human cancer cells in vivo. Nucleic Acids Res. 2015;43(4):2022–32.
13. Zhong Z, Shiue L, Kaplan S, de Lange T. A mammalian factor that binds telomeric TTAGGG repeats in vitro. Mol Cell Biol. 1992;12(11):4834–43.
14. Broccoli D, Smogorzewska A, Chong L, De Lange T. Human telomeres contain two distinct Myb-related proteins, TRF1 and TRF2. Nat Genet. 1997;17:231–5.
15. Fairall L, Chapman L, Moss H, De Lange T, Rhodes D. Structure of the TRFH dimerization domain of the human telomeric proteins TRF1 and TRF2. Mol Cell. 2001;8(2):351–61.
16. Stansel RM, De Lange T, Griffith JD. T-loop assembly in vitro involves binding of TRF2 near the 3′ telomeric overhang. EMBO J. 2001;20(19):5532–40.
17. de Lange T. Shelterin-Mediated Telomere Protection. Annu Rev Genet. 2018;52(1):223–47.
18. Houghtaling BR, Cuttonaro L, Chang W, Smith S. A Dynamic Molecular Link between the Telomere Length Regulator TRF1 and the Chromosome End Protector TRF2. Icarus. 2004;14:1621–31.
19. Li B, Oestreich S, De Lange T. Identification of human Rap1: Implications for telomere evolution. Cell. 2000;101(5):471–83.
20. Lei M, Podell ER, Cech TR. Structure of human POT1 bound to telomeric single-stranded DNA provides a model for chromosome end-protection. Nat Struct Mol Biol. 2004;11(12):1223–9.
21. De Lange T. Shelterin: The protein complex that shapes and safeguards human telomeres. Genes Dev. 2005;19(18):2100–10.
22. Wu P, Takai H, De Lange T. Telomeric 3′ overhangs derive from resection by Exo1 and apollo and fill-in by POT1b-associated CST. Cell [Internet]. 2012;150(1):39–52. Available from: http://dx.doi.org/10.1016/j.cell.2012.05.026
23. Doksani Y, Wu JY, De Lange T, Zhuang X. Super-resolution fluorescence imaging of telomeres reveals TRF2-dependent T-loop formation. Cell [Internet]. 2013;155(2):345. Available from: http://dx.doi.org/10.1016/j.cell.2013.09.048

24. Dimitrova N, de Lange T. Cell Cycle-Dependent Role of MRN at Dysfunctional Telomeres: ATM Signaling-Dependent Induction of Nonhomologous End Joining (NHEJ) in G1 and Resection-Mediated Inhibition of NHEJ in G2. Mol Cell Biol. 2009;29(20):5552–63.
25. Azzalin CM, Reichenbach P, Khoriauli L, Giulotto E, Lingner J. Telomeric Repeat–Containing RNA and RNA Surveillance Factors at Mammalian Chromossome Ends. Science (80-). 2007;318(November):798–801.
26. Schoeftner S, Blasco MA. Developmentally regulated transcription of mammalian telomeres by DNA-dependent RNA polymerase II. Nat Cell Biol. 2008;10(2):228–36.
27. Nergadze SG, Farnung BO, Wischnewski H, Khoriauli L, Vitelli V, Chawla R, et al. CpG-island promoters drive transcription of human telomeres. Rna. 2009;15(12):2186–94.
28. Hu Y, Bennett HW, Liu N, Moravec M, Williams JF, Azzalin CM, et al. RNA – DNA Hybrids Support Recombination-Based Telomere Maintenance in Fission Yeast Yan. Genetics. 2019;213(October):431–47.
29. Victorelli S, Passos JF. Telomeres and Cell Senescence - Size Matters Not. EBioMedicine [Internet]. 2017;21:14–20. Available from: http://dx.doi.org/10.1016/j.ebiom.2017.03.027
30. Bochnam ML, Paeschke K, Zakian VA. DNA secondary structures: stability and function of G-quadruplex structures. Nat Rev Genet. 2012;13(050):770–80.
31. Levy MZ, Allsopp RC, Futcher AB, Greider CW, Harley CB. Telomere end-replication problem and cell aging. J Mol Biol. 1992;225(4):951–60.
32. D 'adda F, Fagagna D, Reaper PM, Clay-Farrace L, Fiegler H, Carr P, et al. A DNA damage checkpoint response in telomere-initiated senescence. Nature. 2003;426(November):194–8.
33. Wright WE, Piatyszek MA, Rainey WE, Byrd W, Shay JW. Telomerase activity in human germline and embryonic tissues and cells. Dev Genet. 1996;18(2):173–9.
34. Greider CW, Blackburn EH. Identification of a specific telomere terminal transferase activity in tetrahymena extracts. Cell. 1985;43(2 PART 1):405–13.
35. Diede SJ, Gottschling DE. Telomerase-mediated telomere addition in vivo requires DNA primase and DNA polymerases α and δ. Cell. 1999;99:723–33.
36. Marcand S, Brevet V, Mann C, Gilson E. Cell cycle restriction of telomere elongation. Curr Biol. 2000;10(8):487–90.
37. Teixeira MT, Arneric M, Sperisen P, Lingner J. Telomere Length Homeostasis Is Achieved via a Switch between Telomerase- Extendible and -Nonextendible States M. Cell [Internet]. 2004;117:323–35. Available from: papers2://publication/uuid/F7231C45-553F-4456-8309-F459A1871F2F
38. Hanahan D, Weinberg RA. Hallmarks of cancer: The next generation. Cell [Internet]. 2011;144(5):646–74. Available from: http://dx.doi.org/10.1016/j.cell.2011.02.013
39. Kim NW, Piatyszek MA, Prowse KR, Harley CB, West MD, Ho PLC, et al. Specific association of human telomerase activity with immortal cells and cancer. Science (80-). 1994;266(5193):2011–5.
40. Bryan TM, Englezou A, Gupta J, Bacchetti S, Reddel RR. Telomere elongation in immortal human cells without detectable telomerase activity. EMBO J. 1995;14(17):4240–8.
41. Heaphy CM, Subhawong AP, Hong SM, Goggins MG, Montgomery EA, Gabrielson E, et al. Prevalence of the alternative lengthening of telomeres telomere maintenance mechanism in human cancer subtypes.

Am J Pathol. 2011;179(4):1608–15.

42. Yeager TR, Neumann AA, Englezou A, Huschtscha LI, Noble JR, Reddel RR. Telomerase-negative immortalized human cells contain a novel type of promyelocytic leukemia (PML) body. Cancer Res. 1999;59(17):4175–9.
43. Draskovic I, Arnoult N, Steiner V, Bacchetti S, Lomonte P, Londoño-Vallejo A. Probing PML body function in ALT cells reveals spatiotemporal requirements for telomere recombination. Proc Natl Acad Sci U S A. 2009;106(37):15726–31.
44. Wu G, Lee WH, Chen PL. NBS1 and TRF1 colocalize at promyelocytic leukemia bodies during late S/G2 phases in immortalized telomerase-negative cells. Implication of NBS1 in alternative lengthening of telomeres. J Biol Chem. 2000;275(39):30618–22.
45. Henson JD, Cao Y, Huschtscha LI, Chang AC, Au AYM, Pickett HA, et al. DNA C-circles are specific and quantifiable markers of alternative- lengthening-of-telomeres activity. Nat Biotechnol [Internet]. 2009;27(12):1181–5. Available from: http://dx.doi.org/10.1038/nbt.1587
46. Cesare AJ, Griffith JD. Telomeric DNA in ALT Cells Is Characterized by Free Telomeric Circles and Heterogeneous t-Loops. Mol Cell Biol. 2004;24(22):9948–57.
47. Bailey SM, Brenneman MA, Goodwin EH. Frequent recombination in telomeric DNA may extend the proliferative life of telemerase-negative cells. Nucleic Acids Res. 2004;32(12):3743–51.
48. Lovejoy CA, Li W, Reisenweber S, Thongthip S, Bruno J, de Lange T, et al. Loss of ATRX, genome instability, and an altered DNA damage response are hallmarks of the alternative lengthening of Telomeres pathway. PLoS Genet. 2012;8(7):12–5.
49. Azzalin CM, Lingner J. Telomere functions grounding on TERRA firma. Trends Cell Biol [Internet]. 2015;25(1):29–36. Available from: http://dx.doi.org/10.1016/j.tcb.2014.08.007
50. Arora R, Lee Y, Wischnewski H, Brun CM, Schwarz T, Azzalin CM. RNaseH1 regulates TERRA-telomeric DNA hybrids and telomere maintenance in ALT tumour cells. Nat Commun [Internet]. 2014;5:1–11. Available from: http://dx.doi.org/10.1038/ncomms6220
51. Silva B, Pentz R, Figueira AM, Arora R, Lee YW, Hodson C, et al. FANCM limits ALT activity by restricting telomeric replication stress induced by deregulated BLM and R-loops. Nat Commun [Internet]. 2019;10(1):1–16. Available from: http://dx.doi.org/10.1038/s41467-019-10179-z
52. Kramara J, Osia B, Malkova A. Break-Induced Replication: The Where, The Why, and The How. Trends Genet [Internet]. 2018;34(7):518–31. Available from: https://doi.org/10.1016/j.tig.2018.04.002
53. Lundblad V, Blackburn EH. An alternative pathway for yeast telomere maintenance rescues est1-senescence. Cell. 1993;73(2):347–60.
54. Le S, Moore JK, Haber JE, Greider CW. RAD50 and RAD51 define two pathways that collaborate to maintain telomeres in the absence of telomerase. Genetics. 1999;152(1):143–52.
55. Chen Q, Ijpma A, Greider CW. Two Survivor Pathways That Allow Growth in the Absence of Telomerase Are Generated by Distinct Telomere Recombination Events. Mol Cell Biol. 2001;21(5):1819–27.
56. Teng SC, Chang J, McCowan B, Zakian VA. Telomerase-independent lengthening of yeast telomeres occurs by an abrupt Rad50p-dependent, Rif-inhibited recombinational process. Mol Cell. 2000;6(4):947–52.
57. Dilley RL, Verma P, Cho NW, Winters HD, Wondisford AR, Greenberg RA. Break-induced telomere

synthesis underlies alternative telomere maintenance. Nature [Internet]. 2016;539(7627):54–8. Available from: http://dx.doi.org/10.1038/nature20099

58. Zhang JM, Yadav T, Ouyang J, Lan L, Zou L. Alternative Lengthening of Telomeres through Two Distinct Break-Induced Replication Pathways. Cell Rep [Internet]. 2019;26(4):955-968.e3. Available from: https://doi.org/10.1016/j.celrep.2018.12.102
59. Roumelioti F, Sotiriou SK, Katsini V, Chiourea M, Halazonetis TD, Gagos S. Alternative lengthening of human telomeres is a conservative DNA replication process with features of break-induced replication . EMBO Rep. 2016;17(12):1731–7.
60. Loe TK, Zhou Li JS, Zhang Y, Azeroglu B, Boddy MN, Denchi EL. Telomere length heterogeneity in ALT cells is maintained by PML-dependent localization of the BTR complex to telomeres. Genes Dev. 2020;34(9–10):650–62.
61. Sobinoff AP, Allen JA, Neumann AA, Yang SF, Walsh ME, Henson JD, et al. BLM and SLX4 play opposing roles in recombination-dependent replication at human telomeres. EMBO J. 2017;36(19):2907–19.
62. Verma P, Dilley RL, Zhang T, Gyparaki MT, Li Y, Greenberg RA. RAD52 and SLX4 act nonepistatically to ensure telomere stability during alternative telomere lengthening. Genes Dev. 2019;33(3–4):221–35.
63. Zhang T, Zhang Z, Shengzhao G, Li X, Liu H, Zhao Y. Strand break-induced replication fork collapse leads to C-circles, C-overhangs and telomeric recombination. PLoS Genet. 2019;15(2).
64. Henson JD, Reddel RR. Assaying and investigating Alternative Lengthening of Telomeres activity in human cells and cancers. FEBS Lett [Internet]. 2010;584(17):3800–11. Available from: http://dx.doi.org/10.1016/j.febslet.2010.06.009
65. Flynn RL, Cox KE, Jeitany M, Wakimoto H, Bryll AR, Ganem NJ, et al. Alternative lengthening of telomeres renders cancer cells hypersensitive to ATR inhibitors. Science (80-). 2015;347(6219):273–7.
66. Suram A, Kaplunov J, Patel PL, Ruan H, Cerutti A, Boccardi V, et al. Oncogene-induced telomere dysfunction enforces cellular senescence in human cancer precursor lesions. EMBO J. 2012;31(13):2839–51.
67. Sfeir A, Kosiyatrakul ST, Hockemeyer D, Macrae SL, Schildkraut CL, Lange T De. Mammalian telomeres resemble fragile sites and require TRF1 for efficient replication. Cell. 2009;138(1):90–103.
68. Cesare AJ, Kaul Z, Cohen SB, Napier CE, Pickett HA, Neumann AA, et al. Spontaneous occurrence of telomeric DNA damage response in the absence of chromosome fusions. Nat Struct Mol Biol [Internet]. 2009;16(12):1244–51. Available from: http://dx.doi.org/10.1038/nsmb.1725
69. Lu R, O'Rourke JJ, Sobinoff AP, Allen JAM, Nelson CB, Tomlinson CG, et al. The FANCM-BLM-TOP3A-RMI complex suppresses alternative lengthening of telomeres (ALT). Nat Commun [Internet]. 2019;10(1). Available from: http://dx.doi.org/10.1038/s41467-019-10180-6
70. Pan X, Drosopoulos WC, Sethi L, Madireddy A, Schildkraut CL, Zhang D. FANCM, BRCA1, and BLM cooperatively resolve the replication stress at the ALT telomeres. Proc Natl Acad Sci U S A. 2017;114(29):E5940–9.
71. Cox KE, Maréchal A, Flynn RL. SMARCAL1 Resolves Replication Stress at ALT Telomeres. Cell Rep. 2016;14(5):1032–40.
72. Ge H, Roeder RG. Purification, cloning, and characterization of a human coactivator, PC4, that mediates

transcriptional activation of class II genes. Cell. 1994;78(3):513–23.

73. Blasco MA, Lee HW, Hande MP, Samper E, Lansdorp PM, DePinho RA, et al. Telomere shortening and tumor formation by mouse cells lacking telomerase RNA. Cell. 1997;91(1):25–34.

74. Akimoto Y, Yamamoto S, Iida S, Hirose Y, Tanaka A, Hanaoka F, et al. Transcription cofactor PC4 plays essential roles in collaboration with the small subunit of general transcription factor TFIIE. Genes to Cells. 2014;19(12):879–90.

75. Janowski R, Niessing D. The large family of PC4-like domains–similar folds and functions throughout all kingdoms of life. RNA Biol [Internet]. 2020;17(9):1228–38. Available from: https://doi.org/10.1080/15476286.2020.1761639

76. Werten S, Langen FWM, Van Schaik R, Timmers HTM, Meisterernst M, Van Der Vliet PC. High-affinity DNA binding by the C-terminal domain of the transcriptional coactivator PC4 requires simultaneous interaction with two opposing unpaired strands and results in helix destabilization. J Mol Biol. 1998;276(2):367–77.

77. Werten S, Stelzer G, Goppelt A, Langen FM, Gros P, Timmers HTM, et al. Interaction of PC4 with melted DNA inhibits transcription. EMBO J. 1998;17(17):5103–11.

78. Fukuda A, Tokonabe S, Hamada M, Matsumoto M, Tsukui T, Nogi Y, et al. Alleviation of PC4-mediated transcriptional repression by the ERCC3 helicase activity of general transcription factor TFIIH. J Biol Chem. 2003;278(17):14827–31.

79. Wu SY, Chiang CM. Properties of PC4 and an RNA polymerase II complex in directing activated and basal transcription in vitro. J Biol Chem. 1998;273(20):12492–6.

80. Werten S, Wechselberger R, Boelens R, Van Der Vliet PCD, Kaptein R. Identification of the single-stranded DNA binding surface of the transcriptional coactivator PC4 by NMR. J Biol Chem. 1999;274(6):3693–9.

81. Batta K, Kundu TK. Activation of p53 Function by Human Transcriptional Coactivator PC4: Role of Protein-Protein Interaction, DNA Bending, and Posttranslational Modifications. Mol Cell Biol. 2007;27(21):7603–14.

82. Gao J, Zybailov BL, Byrd AK, Griffin WC, Chib S, Mackintosh SG, et al. Yeast transcription co-activator Sub1 and its human homolog PC4 preferentially bind to G-quadruplex DNA. Chem Commun [Internet]. 2015;51(33):7242–4. Available from: http://dx.doi.org/10.1039/C5CC00742A

83. Griffin WC, Gao J, Byrd AK, Chib S, Raney KD. A biochemical and biophysical model of G-quadruplex DNA. J Biol Chem. 2017;292(23):9567–82.

84. Ge H. UPA, a universal protein array system for quantitative detection of protein-protein, protein-DNA, protein-RNA and protein-ligand interactions. Nucleic Acids Res. 1999;28(2).

85. Hudson WH, Ortlund EA. The structure, function and evolution of proteins that bind DNA and RNA. Nat Rev Mol Cell Biol. 2014;15(11):749–60.

86. Brandsen J, Werten S, Van Der Vliet PC, Meisterernst M, Kroon J, Gros P. C-terminal domain of transcription cofactor PC4 reveals dimeric ssDNA binding site. Nat Struct Biol. 1997;4(11):900–3.

87. Werten S, Moras D. A global transcription cofactor bound to juxtaposed strands of unwound DNA. Nat Struct Mol Biol. 2006;13(2):181–2.

88. Huang J, Zhao Y, Liu H, Huang D, Cheng X, Zhao W, et al. Substitution of tryptophan 89 with tyrosine

switches the DNA binding mode of PC4. Sci Rep. 2015;5(Figure 1):1–6.

89. Malik S, Guermah M, Roeder RG. A dynamic model for PC4 coactivator function in RNA polymerase II transcription. Proc Natl Acad Sci U S A. 1998;95(5):2192–7.

90. Ge H, Zhao Y, Chait BT, Roeder RG. Phosphorylation negatively regulates the function of coactivator PC4. Proc Natl Acad Sci U S A. 1994;91(26):12691–5.

91. Kaiser K, Stelzer G, Meisterernst M. The coactivator p15 (PC4) initiates transcriptional activation during TFIIA-TFIID-promoter complex formation. EMBO J. 1995;14(14):3520–7.

92. Kumar BRP, Swaminathan V, Banerjee S, Kundu TK. p300-mediated Acetylation of Human Transcriptional Coactivator PC4 Is Inhibited by Phosphorylation. J Biol Chem. 2001;276(20):16804–9.

93. Calvo O, Manley JL. Evolutionarily conserved interaction between CstF-64 and PC4 links transcription, polyadenylation, and termination. Mol Cell. 2001;7(5):1013–23.

94. Wang Z, Roeder RG. DNA topoisomerase I and PC4 can interact with human TFIIIC to promote both accurate termination and transcription reinitiation by RNA polymerase III. Mol Cell. 1998;1(5):749–57.

95. Fukuda A, Nakadai T, Shimada M, Tsukui T, Matsumoto M, Nogi Y, et al. Transcriptional Coactivator PC4 Stimulates Promoter Escape and Facilitates Transcriptional Synergy by GAL4-VP16. Mol Cell Biol. 2004;24(14):6525–35.

96. Pan ZQ, Ge H, Amin AA, Hurwitz J. Transcription-positive cofactor 4 forms complexes with HSSB (RPA) on single-stranded DNA and influences HSSB-dependent enzymatic synthesis of simian virus 40 DNA. J Biol Chem. 1996;271(36):22111–6.

97. Mortusewicz O, Roth W, Li N, Cardoso MC, Meisterernst M, Leonhardt H. Recruitment of RNA polymerase II cofactor PC4 to DNA damage sites. J Cell Biol. 2008;183(5):769–76.

98. Das C, Hizume K, Batta K, Kumar BRP, Gadad SS, Ganguly S, et al. Transcriptional Coactivator PC4, a Chromatin-Associated Protein, Induces Chromatin Condensation. Mol Cell Biol. 2006;26(22):8303–15.

99. Das C, Gadad SS, Kundu TK. Human Positive Coactivator 4 Controls Heterochromatinization and Silencing of Neural Gene Expression by Interacting with REST/NRSF and CoREST. J Mol Biol [Internet]. 2010;397(1):1–12. Available from: http://dx.doi.org/10.1016/j.jmb.2009.12.058

100. Wang J-Y, Sarker AH, Cooper PK, Volkert MR. The Single-Strand DNA Binding Activity of Human PC4 Prevents Mutagenesis and Killing by Oxidative DNA Damage. Mol Cell Biol. 2004;24(13):6084–93.

101. Mortusewicz O, Evers B, Helleday T. PC4 promotes genome stability and DNA repair through binding of ssDNA at DNA damage sites. Oncogene [Internet]. 2016;35(6):761–70. Available from: http://dx.doi.org/10.1038/onc.2015.135

102. Batta K, Yokokawa M, Takeyasu K, Kundu TK. Human Transcriptional Coactivator PC4 Stimulates DNA End Joining and Activates DSB Repair Activity. J Mol Biol [Internet]. 2009;385(3):788–99. Available from: http://dx.doi.org/10.1016/j.jmb.2008.11.008

103. Banerjee S, Kumar BRP, Kundu TK. General Transcriptional Coactivator PC4 Activates p53 Function. Mol Cell Biol. 2004;24(5):2052–62.

104. Rajagopalan S, Andreeva A, Teufel DP, Freund SM, Fersht AR. Interaction between the transactivation domain of p53 and PC4 exemplifies acidic activation domains as single-stranded DNA mimics. J Biol Chem. 2009;284(32):21728–37.

105. Chen L, Du C, Wang L, Yang C, Zhang JR, Li N, et al. Human positive coactivator 4 (PC4) is involved

in the progression and prognosis of astrocytoma. J Neurol Sci. 2014;346(1–2):293–8.

106. Hu X, Zhang C, Zhang Y, Hong CS, Chen W, Shen W, et al. Down regulation of human positive coactivator 4 suppress tumorigenesis and lung metastasis of osteosarcoma. Oncotarget. 2017;8(32):53210–25.

107. Zhang T, Liu X, Chen X, Wang J, Wang Y, Qian D, et al. Inhibition of PC4 radiosensitizes non-small cell lung cancer by transcriptionally suppressing XLF. Cancer Med. 2018;7(4):1326–37.

108. Luo P, Zhang C, Liao F, Chen L, Liu Z, Long L, et al. Transcriptional positive cofactor 4 promotes breast cancer proliferation and metastasis through c-Myc mediated Warburg effect. Cell Commun Signal. 2019;17(1):1–13.

109. Zhang J, Lee D, Dhiman V, Jiang P, Xu J, McGillivray P, et al. An integrative ENCODE resource for cancer genomics. Nat Commun. 2020;11(1).

110. Scheibe M, Arnoult N, Kappei D, Buchholz F, Decottignies A, Butter F, et al. Quantitative interaction screen of telomeric repeatcontaining RNA reveals novel TERRA regulators. Genome Res. 2013;23(12):2149–57.

111. Pérez-Martínez L, Öztürk M, Butter F, Luke B. Npl3 stabilizes R-loops at telomeres to prevent accelerated replicative senescence. EMBO Rep. 2020;21(3):1–12.

112. Lee YW, Arora R, Wischnewski H, Azzalin CM. TRF1 participates in chromosome end protection by averting TRF2-dependent telomeric R loops. Nat Struct Mol Biol. 2018;25(2):147–53.

113. Grudic A, Jul-Larsen Å, Haring SJ, Wold MS, Lønning PE, Bjerkvig R, et al. Replication protein A prevents accumulation of single-stranded telomeric DNA in cells that use alternative lengthening of telomeres. Nucleic Acids Res. 2007;35(21):7267–78.

114. Olson E, Nievera CJ, Klimovich V, Fanning E, Wu X. RPA2 is a direct downstream target for ATR to regulate the S-phase checkpoint. J Biol Chem. 2006;281(51):39517–33.

115. Podhorecka M, Skladanowski A, Bozko P. H2AX phosphorylation: Its role in DNA damage response and cancer therapy. J Nucleic Acids. 2010;2010.

116. Holt SE, Wright WE, Shay JW. Regulation of Telomerase Activity in Cell Lines. 1996;16(6):2932–9.

117. Patel A, Joshi G, Fu Y, Shaju S, Messina A. Telomere elongation and Telomerase activity in Normal and Cancer cell lines: HEK-293, HeLa and A549. 2017;100446.

118. Norbury CJ, Hickson ID. Cellular responses to DNA damage. Annu Rev. 2001;41:367–401.

119. Fadeel B, Orrenius S. Apoptosis: A basic biological phenomenon with wide-ranging implications in human disease. J Intern Med. 2005;258(6):479–517.

120. Glick D, Barth S, Macleod KF. Autophagy: Cellular and molecular mechanisms. J Pathol. 2010;221(1):3–12.

121. Gobeil S, Boucher CC, Nadeau D, Poirier GG. Characterization of the necrotic cleavage of poly (ADP-ribose) polymerase (PARP-1): Implication of lysosomal proteases. Cell Death Differ. 2001;8(6):588–94.

122. Runwal G, Stamatakou E, Siddiqi FH, Puri C, Zhu Y, Rubinsztein DC. LC3-positive structures are prominent in autophagy-deficient cells. Sci Rep [Internet]. 2019;9(1):1–14. Available from: http://dx.doi.org/10.1038/s41598-019-46657-z

123. Singh A, Xu Y. The Cell Killing Mechanisms of Hydroxyurea. 2016;

7. Annexes

Table 7.1 List of DsiRNAs mRNA target sequence

siRNA	Sequence
siPC4a	5'- TGA GTG AAG CTA ATT GTC AAC TTT A -3'
siPC4b	5'- ACA UUG AUG AUG CAG UAA GAA AAC T -3'
siPC4c	5'- GAU UCU GAC AGU GAG GUU GAC AAA A -3'
siRPA70	5'- AAC ACU CUA UCC UCU UUC AUG UUG G -3'
siFANCM	5′- GGA TGT TTA GGA GAA CAA AGA GCT A -3′
siRNAseH1	5'- CUU GAA UUU CCG CUC UUU GGU UUG UCU -3'
siTRF1c	5'- CUU UCU UUC UUA UUA AGG UCU UGU UGC -3'
siCt	5'- AAT TCT CCG AAC GTG TCA CGT -3'

Table 7.2 List of antibodies used for western blotting

Antibody	Source and Reference	Dilution
Mouse monoclonal anti-FANCM	CV5.1	1:1000
Rabbit polyclonal anti-RPA70	Bethyl Laboratories, A300-241A	1:2000
Mouse monoclonal anti-beta Actin	Abcam, ab8224	1:5000
Mouse monoclonal anti-Golgin 97	Molecular Probes, A-21270	1:5000
Rabbit polyclonal anti-RNaseH1	GeneTex, GTX117624	1:500
Rabbit polyclonal anti-PARP	Cell Signaling, 9542	1:1000
Sheep polyclonal anti-TRF1	R&D Systems, AF5300	1:1000
Rabbit polyclonal anti-PC4	Bethyl Laboratories, A301-161A-M	1:1000
Rabbit polyclonal anti-FLAG	SIGMA, F7425-0.2mg	1:4000
Rabbit monoclonal anti-POT1	Abcam, ab124784	1:2000
Rabbit polyclonal anti-TRF2	Novus Biologicals, NB110-57130	1:2000
Mouse monoclonal anti-TPP1	Abnova, H00001200-M01	1:2000
Rabbit polyclonal anti-Rap1	Bethyl Laboratories, A300-306A	1:2000
Mouse monoclonal anti-TIN2	Santa Cruz Biotechnology, 59B388	1:500
Rabbit polyclonal anti-LC3B	Kindly provided by Sergio Almeida, iMM, Lisbon, Portugal	1:1000
Goat anti-mouse IgG	Bethyl Laboratories, A90-116P	1:2000
Goat anti-rabbit IgG	Bethyl Laboratories, A120-101P	1:2000
Donkey anti-sheep IgG	Novus Biologicals, NBP1-75437	1:3000

Table 7.3 List of antibodies used for immunofluorescence

Antibody	Source and Reference	Dilution
Mouse monoclonal anti-TRF2	Millipore, 05-521	1:500
Rabbit polyclonal anti-TRF2	Novus Biologicals, NB110-57130	1:500
Rabbit polyclonal anti-PC4	Bethyl Laboratories, A301-161A-M	1:100
Mouse monoclonal anti-FLAG	Sigma-Aldrich, F1804	1:1000
Rabbit polyclonal anti-pRPA32 pSer 33	Bethyl Laboratories, A300-246A	1:1000
Mouse monoclonal anti-γH2AX	Upstate (Millipore), 05-636	1:1000
Alexa Fluor 568-conjugated donkey anti-mouse IgGs	Thermo Fisher Scientific, A10037	1:1000
Alexa Fluor 488-conjugated donkey anti-rabbit IgGs	Thermo Fisher Scientific, A21206	1:1000
Alexa Fluor 488-conjugated donkey anti-mouse IgGs	Thermo Fisher Scientific, A21202	1:1000
Alexa Fluor 568-conjugated donkey anti-rabbit IgGs	Thermo Fisher Scientific, A10042	1:1000

Table 7.4 List of oligonucleotide sequences used for RT-qPCR

Primer	Sequence
TRF1 Forward	5’ – TCT CTC TTT GCC GAG CTT TCC – 3’
TRF1 Reverse	5’ – ACT GGC AAG CTG TTA GAC TGG AT – 3’
U6 Forward	5’ – CTC GCT TCG GCA GCA CAT ATA – 3’
U6 Reverse	5’ – GGA ACG CTT CAC GAA TTT GCG T – 3’

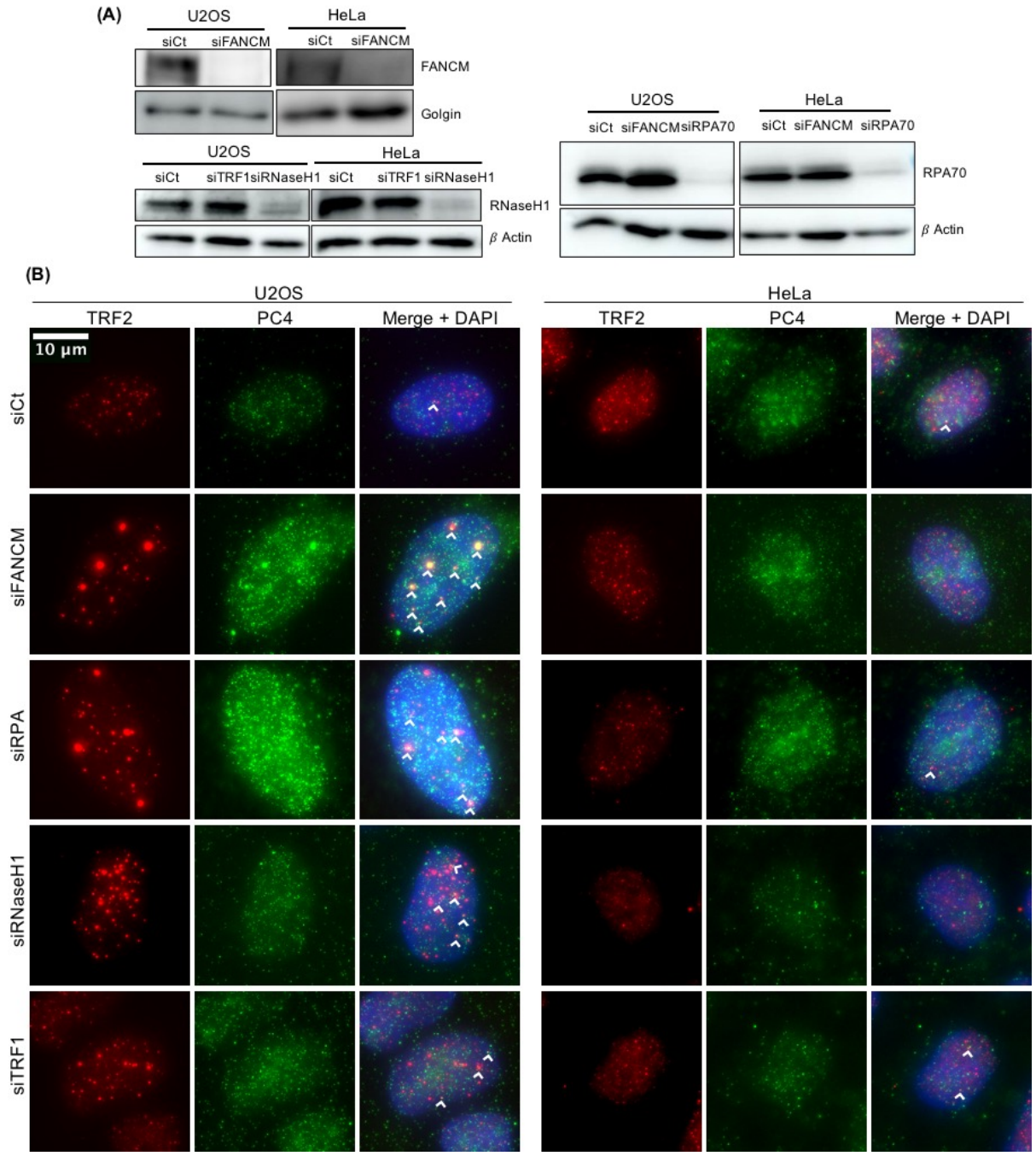

Figure 7.1 PC4 recruitment to telomeres due to stress, related to figure 4.5 and 4.6. (A) Western blotting analysis of U2OS and HeLa after 48 h or 72 h transfection with 20 nM of siCt, siFANCM, siRPA70 or siRNaseH1; (B) A total of at least 100 nuclei from 3 independent experiments were analyzed for each sample. Examples of PC4 immunostaining (green) combined with TRF2 immunostaining (red) in U2OS and HeLa. In the merge panel, DAPI-stained DNA is also shown (blue). Arrows indicate co-localizations between PC4 and TRF2.

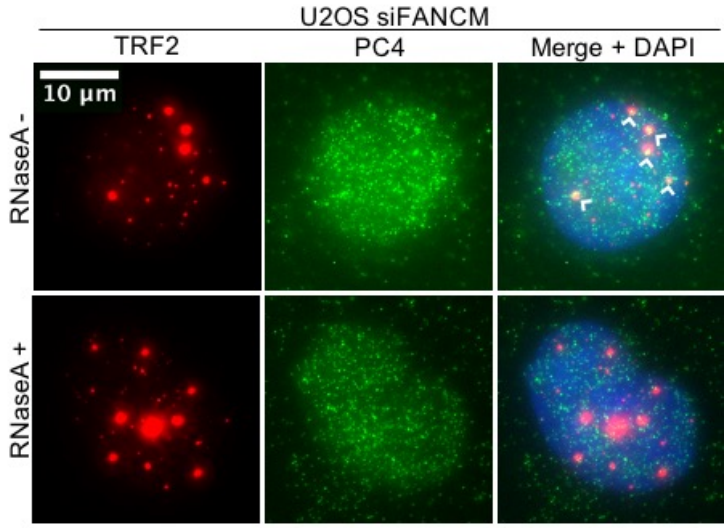

Figure 7.2 PC4 recruitment mediated by RNA in U2OS, related to figure 4.8. Examples of PC4 immunostaining (green) combined with TRF2 immunostaining (red) in U2OS siFANCM without treatment with RNaseA (-) and with treatment before fixation (+). In the merge panel, DAPI-stained DNA is also shown (blue). Arrows indicate co-localizations between PC4 and TRF2

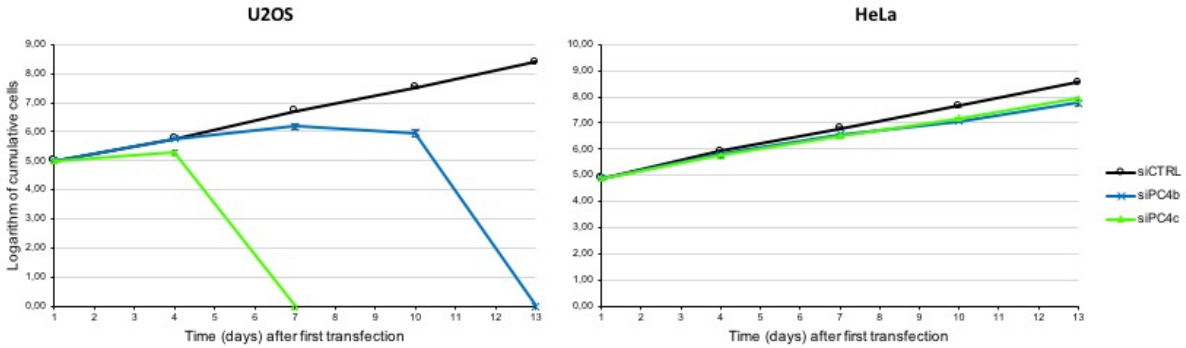

Figure 7.3 Growth curves in U2OS and HeLa, related to figure 4.12. Cellular proliferation of U2OS and HeLa after transfection with 30 nM of siCt, siPC4b or siPC4c every 3 days. Cumulative cell numbers are expressed in a logarithmic transformation of base 10. Data points and error bars are means and SDs from 3 independent experiments.